

Dalton Transactions

Accepted Manuscript



This is an *Accepted Manuscript*, which has been through the Royal Society of Chemistry peer review process and has been accepted for publication.

Accepted Manuscripts are published online shortly after acceptance, before technical editing, formatting and proof reading. Using this free service, authors can make their results available to the community, in citable form, before we publish the edited article. We will replace this *Accepted Manuscript* with the edited and formatted *Advance Article* as soon as it is available.

You can find more information about *Accepted Manuscripts* in the [Information for Authors](#).

Please note that technical editing may introduce minor changes to the text and/or graphics, which may alter content. The journal's standard [Terms & Conditions](#) and the [Ethical guidelines](#) still apply. In no event shall the Royal Society of Chemistry be held responsible for any errors or omissions in this *Accepted Manuscript* or any consequences arising from the use of any information it contains.

Synthesis, Protonation Equilibrium and Peculiar Thermal Decomposition

Behavior of *cyclo*-tri- μ -imidotetraphosphate

Hideshi Maki*, Kazuomi Ryousi, Hiroyuki Nariai, Minoru Mizuhata

Department of Chemical Science and Engineering, Graduate School of Engineering, Kobe University,
1-1 Rokkodai-cho, Nada-ku, Kobe 657-8501, Japan

CORRESPONDING AUTHOR FOOTNOTE

Authors to whom correspondence should be addressed. E-mail: maki@kobe-u.ac.jp

Abstract

The synthesis and isolation of sodium salt of *cyclo*-tri- μ -imidotetraphosphate, i.e., $\text{Na}_4\text{cP}_4\text{O}_9(\text{NH})_3 \cdot \text{H}_2\text{O}$, were achieved by the hydrolysis of $\text{Na}_4\text{cP}_4\text{O}_8(\text{NH})_4 \cdot 2\text{H}_2\text{O}$ under very weak acidic condition, i.e., 0.2 mol L^{-1} propionic acid and pH-controlled recrystallization procedure. The purity of $\text{Na}_4\text{cP}_4\text{O}_9(\text{NH})_3 \cdot \text{H}_2\text{O}$ was improved from 2% to 95% by the pH-controlled recrystallization of only two times. The first protonation constants of a series of *cyclo*- μ -imidotetraphosphate anions, i.e., $\text{cP}_4\text{O}_{12-n}(\text{NH})_n^{4-}$ ($n = 0, 2, 3, 4$), were determined by potentiometric titration and ^{31}P NMR chemical shift measurements in aqueous solution. Regardless of the paucity of the purity of *trans*- $\text{cP}_4\text{O}_{10}(\text{NH})_2^{4-}$ anion, the protonation processes of all anions may be evaluated accurately without any previous purification, because the NMR signals corresponding to $\text{cP}_4\text{O}_{12-n}(\text{NH})_n^{4-}$ ($n = 0, 2, 3, 4$) anions are well resolved. The logarithmic first protonation constants increase with an increase "linearly" in the number of imino groups which constitute the ligand molecules. Macroscopic protonation reactions could be divided into three microscopic protonation processes for $-\text{O}-\text{PO}_2-\text{O}-$, $-\text{O}-\text{PO}_2-\text{NH}-$, and

$\text{-NH-PO}_2\text{-NH-}$ groups. The basicity of $\text{-NH-PO}_2\text{-NH-}$ group is especially high, because the delocalization of H^+ ions by lactam-lactim tautomerism on the whole ring molecule of $\text{cP}_3\text{O}_6(\text{NH})_3$ and $\text{cP}_4\text{O}_8(\text{NH})_4$ enhance the protonation of these ligands. In addition, also the concurrent change observed in the ^{31}P NMR chemical shift values of the phosphorus nuclei in the $\text{-O-PO}_2\text{-NH-}$ and $\text{-NH-PO}_2\text{-NH-}$ groups of $\text{cP}_4\text{O}_9(\text{NH})_3^{4-}$ anion suggested the effect of the lactam-lactim tautomerism. The intrinsic ^{31}P NMR chemical shifts for the central phosphorus nuclei for $\text{-O-PO}_2\text{-O-}$, $\text{-O-PO}_2\text{-NH-}$, and $\text{-NH-PO}_2\text{-NH-}$ groups show a good proportional relationship with the number of nitrogen atoms bonded to the central phosphorus atoms. Two types of imino groups with mutually dissimilar chemical environments which are present in the $\text{Na}_4\text{cP}_4\text{O}_9(\text{NH})_3$ molecule, that is, $\text{-O-PO}_2\text{-NH-PO}_2\text{-NH-}$ and $\text{-NH-PO}_2\text{-NH-PO}_2\text{-NH-}$, brought about a two-stage pyrolytic elimination of imino groups from the initial stage of combustion over a wide temperature range.

Keywords:

imidophosphate, imino group, flame retardant, protonation, pH-controlled recrystallization, potentiometric titration, ^{31}P NMR, tautomerism, lactam-lactim tautomerism, proton conductor,

MANUSCRIPT TEXT

1. Introduction

A series of imidophosphates and ammonium phosphate, as phosphorus-nitrogen compounds, have long been used as chemical fertilizers.¹⁻⁴ In recent years, they have also been applied to flame retardants for organic materials such as various plastics, painting materials, and textiles.⁵⁻¹⁰ Organic materials are essential in our daily lives in these days, however, they have the significant disadvantage of being highly flammable. In order to ameliorate this disadvantage, organic materials are subjected to flameproofing treatment; i.e., the addition or application of a halogen-based flame retardant. During combustion, however, halogen-based flame retardants often generate toxic halogen gas and hydrogen

halide gas. Concerns have also recently been raised over the risk of the release of endocrine disruptors which molecular structure is similar to the halogen-based flame retardants, such as dioxins.^{11–17} There is consequently increasing interest in non-halogen-based flame retardants, such as inorganic phosphate flame retardants. In particular, imidophosphate containing imino groups in the molecular skeleton is attracting considerable attention.^{18–21}

In the initial stage of combustion, phosphate flame retardants exhibit the following flame retardant effect.^{22–25} First, cyclic polyphosphates formed because of the dehydration condensation of the phosphoric acids which were generated by pyrolysis of the phosphate flame retardants. The pyrolysis reactions to the phosphoric acids and the evaporation of water which is accompanied by the dehydration condensation of the phosphoric acids absorb exotherm in the initial stage of the combustion. Additionally, these phosphoric acids and cyclic polyphosphates cover the surface of the combustibles and flame resistance is exerted. In addition, the formed cyclic phosphoric acids promote the carbonization by the dehydration of the combustible materials, and the generated carbonization layer intercepts the supply of oxygen to the combustibles and the flame retardant effect is enhanced. In particular, it is expected that the imidophosphates especially raises the flame retardant effect, since the generation of nonflammable gas which is accompanied by the pyrolytic elimination of the imino groups further intercepts the supply of oxygen from the atmosphere to the flammable material.^{26–28} Especially, there is an advantage that the flame retardants is hard to elute to the environment because the imino groups decrease the solubility to water of the compound.²⁹ Furthermore, in the *cyclo-tri-μ*-imidotetraphosphate, $\text{Na}_4\text{P}_4\text{O}_9(\text{NH})_3$ as shown in Fig. S1, which was synthesized in this study, two types of imino groups with mutually dissimilar chemical environments are present. When we examine the bridging atoms except phosphorus atoms, the following characteristics are noted: (1) an imino group ($-\text{O}-\text{PO}_2-\text{NH}-\text{PO}_2-\text{NH}-$) adjacent to one bridging nitrogen atom and (2) an imino group ($-\text{NH}-\text{PO}_2-\text{NH}-\text{PO}_2-\text{NH}-$) adjacent to two bridging nitrogen atoms are present in an $\text{Na}_4\text{P}_4\text{O}_9(\text{NH})_3$ molecule. This is a unique feature found only in the $\text{Na}_4\text{P}_4\text{O}_9(\text{NH})_3$ among the various short-chain

imidophosphate and *cyclo*- μ -imidophosphate compounds which have been reported. Hence it can be expected that $\text{Na}_4\text{CP}_4\text{O}_9(\text{NH})_3$ may cause a multistage pyrolytic elimination of imino groups and exhibit unique flame retardant properties.

The chemical stabilities of imidophosphates are not high, and in particular, they are more easily hydrolyzed than halogen-based flame retardants.^{30–32} Thus, a series of imidophosphates has not been studied to a significant extent in the past. In recent years, however, the addition of a specific metal ion to imidophosphates has been shown to greatly improve their low hydrolytic stability,^{33–35} resulting in renewed industrial applications which have attracted considerable attention. It is likely that the acid dissociation and complexation equilibria of imidophosphates are closely related to this improvement, although the detailed mechanism is yet to be understood.

There have been several studies on the acid dissociation, complex formation and pyrolysis behaviors of short-chain imidophosphates and *cyclo*- μ -imidotriphosphates as six-membered compounds.^{36–42} On the other hand, except for *cyclo*-tetra- μ -imidotetraphosphate anions as shown in Fig. S1,^{43,44} all four bridging atoms of which are nitrogen atoms, neither synthesis nor isolation has been reported for a series of *cyclo*- μ -imidotetraphosphates as an eight-membered compound. A series of *cyclo*- μ -imidotetraphosphate anions consists of five types of anions as shown in Fig. S1, and *cyclo*-di- μ -imidotetraphosphate anion consists of two *cis-trans* isomers. Thus, a series of *cyclo*- μ -imidotetraphosphate anions is likely to exhibit unique and various acid dissociation and complex formation behaviors, as well as peculiar thermal behaviors, and are expected to be applied to functional chemical materials.

As for the *cyclo*-mono- μ -imidotriphosphate and *cyclo*-di- μ -imidotriphosphate anions which include bridging oxygen atom in the cyclic molecular skeleton, the P–O bonding is easily cleaved by hydrolysis which is caused by the nucleophilic attack from water molecules.^{45–51} Consequently, the *cyclo*-di- μ -imidotriphosphate sodium salt, $\text{Na}_3\text{CP}_3\text{O}_7(\text{NH})_2$, which one of the bridging nitrogen atoms in

cyclo-tri- μ -imidotriphosphate sodium salt, $\text{Na}_3\text{cP}_3\text{O}_6(\text{NH})_3$, was replaced by an oxygen atom is applied to a starting material for the synthesis of diimidotriphosphate sodium salt, $\text{Na}_5\text{P}_3\text{O}_8(\text{NH})_2$, which has short chain molecular structure.^{37,38,52} Similarly, $\text{Na}_4\text{cP}_4\text{O}_9(\text{NH})_3$ is expected to be used as a starting material for the synthesis of $\text{Na}_6\text{P}_4\text{O}_{10}(\text{NH})_3$. In this study, a novel method and pH-controlled recrystallization for the synthesis of $\text{Na}_4\text{cP}_4\text{O}_9(\text{NH})_3$ was developed, and the dependence of the protonation equilibria of various *cyclo*- μ -imidotetraphosphate anions, $\text{cP}_4\text{O}_{12-n}(\text{NH})_n^{4-}$ ($n = 0, 2, 3, 4$), on the number of imino groups which constitute the ligand molecules was investigated by potentiometric titrations and ^{31}P NMR measurements. Furthermore, thermal decomposition behavior of $\text{Na}_4\text{cP}_4\text{O}_9(\text{NH})_3$ was clarified by TG-DTA and X-ray powder diffractometry to evaluate its flame retardant performance.

2. Experimental

2.1. Chemicals

Chemicals used. All chemicals used in this work were of analytical grade and purchased from Wako Pure Chemical Industries, Ltd. As supporting electrolyte for the determinations of the protonation constants of the ligands, analytical grade of NaNO_3 (Merck Co. Ltd., 99%) was used without further purification. A standard NaNO_3 stock solution was prepared at about $3.0 \text{ mol}\cdot\text{L}^{-1}$ with the distilled water after deionization. A portion of the stock solution was dried perfectly at 110°C at least 5 days, thus the molalities of the stock solution were determined gravimetrically. A HNO_3 stock solution was prepared at about $0.25 \text{ mol}\cdot\text{L}^{-1}$ from an analytical grade of HNO_3 with the distilled water after deionization and was standardized by a titration with KHCO_3 .⁵³ A carbonate-free alkaline stock solution was prepared at about $1.0 \text{ mol}\cdot\text{L}^{-1}$ by dilution of a plastic ampoule of CO_2 -free NaOH thick aqueous solution (Merck Co. Ltd., No.109959, 99%) with CO_2 -free water which had been boiled at

least 15 min under N_2 atmosphere. The stock solution was checked periodically by Gran's procedure^{54,55}, and the carbonate was under 0.2% of the NaOH present.

Synthesis of $Na_4cP_4O_8(NH)_4 \cdot 2H_2O$. Tetrasodium *cyclo*-tetra- μ -imidotetraphosphate dihydrate, $Na_4cP_4O_8(NH)_4 \cdot 2H_2O$ ($Na_4cP_4O_8(NH)_4$), which was the starting material for the synthesis of tetrasodium *cyclo*-tri- μ -imidotetraphosphate monohydrate, $Na_4cP_4O_9(NH)_3 \cdot H_2O$ ($Na_4cP_4O_9(NH)_3$), was prepared by an improvement^{43,44} of the previously reported method^{43,44} as illustrated in Scheme 1. 125 g of phosphorous pentachloride, PCl_5 , was dissolved in 320 mL of chlorobenzene, C_6H_5Cl , in a three-necked round-bottom flask at 132 °C. 50 g of ammonium chloride, NH_4Cl , which was ground in detail with a ball mill after 12 hours desiccation at 110 °C was added to the C_6H_5Cl solution of PCl_5 . This mixture solution was reacted at 132 °C for 24 h with stirring at a speed of 800 rpm. After cooling at room temperature, unreacted NH_4Cl was filtrated out from the reaction solution, and the separation of reaction mixture from the filtrate was carried out by distillation under reduced pressure. After cooling of an oily residue including needle-like crystal at room temperature, 20 g of the mixture of hexachlorocyclotriphosphazene (phosponitrilic chloride trimer), $(PNCl_2)_3$, and octachlorocyclotetraphosphazene (phosponitrilic chloride tetramer), $(PNCl_2)_4$, as shown in Fig. S1 as needle-like crystals was filtered off by suction filtration, and washed with acetone in order to remove unreacted PCl_5 . The mixture of $(PNCl_2)_3$ and $(PNCl_2)_4$ was dissolved in 80 mL of 1,4-dioxane in a three-necked round-bottom flask at 45 °C. 100 g of sodium acetate was dissolved in 160 mL of water. This solution was heated to 45 °C and then added to the mixture of $(PNCl_2)_3$ and $(PNCl_2)_4$ solution. This solution was reacted at 45 °C for 4 h with stirring at a speed of 90 rpm. After standing overnight in a refrigerator, a white precipitate of a mixture of trisodium *cyclo*-tri- μ -imidotriphosphate tetrahydrate, $Na_3cP_3O_6(NH)_3 \cdot 4H_2O$, and $Na_4cP_4O_8(NH)_4 \cdot 2H_2O$ formed in the solution. After suction filtration of the solution, the precipitate was dissolved in 200 mL of water. The impurities were removed by the suction filtration, and suitable amount of acetone was put into the filtrate. $Na_4cP_4O_8(NH)_4 \cdot 2H_2O$ as a white

precipitate was filtered off and washed with 50 vol% aqueous ethanol and then 100 vol% acetone, and dried in air. The total yield was 22 g, 33%. The purity was determined by HPLC and ^{31}P NMR and was found to be over 97%. The HPLC measurements were carried out as a previous report,⁵⁶ and the ^{31}P NMR spectra were obtained by a Bruker DPX-250 (5.87T) superconducting Fourier-transform pulse NMR spectrometer with a 10 mm tunable broad-band probe which was operated at 101.258 MHz.

Synthesis of $\text{Na}_4\text{cP}_4\text{O}_{12}\cdot 4\text{H}_2\text{O}$. Tetrasodium *cyclo*-tetrphosphate tetrahydrate, $\text{Na}_4\text{cP}_4\text{O}_{12}\cdot 4\text{H}_2\text{O}$ ($\text{Na}_4\text{cP}_4\text{O}_{12}$), was prepared by an improvement of the previously reported method.⁵⁷ To prevent the formation of linear poly sodium phosphates, all the experiment were carried out under 10 °C. 50 g of phosphorus pentoxide, P_2O_5 , was gradually added to 300 mL of water by stirring and this mixture was placed on ice, and 30 wt% sodium hydroxide aqueous solution was added until pH 7. Then 500 mL of acetone was put into the solution, and the crude product as a white precipitate was filtered off and dissolved in 300 mL of water. The impurities were removed by the suction filtration, and 500 mL of acetone was put into the filtrate. $\text{Na}_4\text{cP}_4\text{O}_{12}\cdot 4\text{H}_2\text{O}$ as a white precipitate was filtered off and washed with 50 vol% aqueous ethanol and then 100 vol% acetone, and dried in air. The total yield was 43 g, 51%.

Purities of chemicals. The purity of $\text{Na}_4\text{cP}_4\text{O}_{12-n}(\text{NH})_n$ ($n = 0, 3, 4$) was determined by HPLC and ^{31}P NMR as described above, and was found to be over 97%. The elemental analysis for $\text{Na}_4\text{cP}_4\text{O}_9(\text{NH})_3\cdot x\text{H}_2\text{O}$ was carried out as follows: the flame atomic absorption method for elemental Na, the colorimetrically with a Mo(V)–Mo(VI) reagent for elemental P, the Kjeldahl method for elemental N, and the observation of weight loss by desorption of crystal water by the heat treatment to 200 °C with a thermogravimetric (TG) measurement for H_2O .

2.2. Potentiometric titrations

First protonation constants of $\text{cP}_4\text{O}_{12-n}(\text{NH})_n^{4-}$ ($n = 0, 3, 4$) were determined by potentiometric titrations. All titration procedures were automatically carried out with an APB-510 automatic piston burette (Kyoto Electronics Manufacturing Co., Ltd.) which was controlled by a personal computer at $25.0 \pm 0.5^\circ\text{C}$ under N_2 atmosphere. A potentiometer (Orion 720A Ionalyzer) equipped with a glass electrode (Orion 91-01) and a single junction reference electrode (Orion 90-02) was used for a potentiometric titration. 20 cm^3 solutions of $0.0025 \text{ mol}\cdot\text{L}^{-1} \text{Na}_4\text{cP}_4\text{O}_{12-n}(\text{NH})_n$ ($n = 0, 3, 4$) + $0.1 \text{ mol}\cdot\text{L}^{-1} \text{NaNO}_3$ were titrated overall by a solution of $0.01 \text{ mol}\cdot\text{L}^{-1} \text{HNO}_3$ + $0.1 \text{ mol}\cdot\text{L}^{-1} \text{NaNO}_3$. The electrochemical cell for potentiometric titrations in this work was illustrated in Fig. S2. Before and after the titrations of the sample solutions, the glass electrode was calibrated as a hydrogen concentration probe by titrating known amounts of HNO_3 with CO_2 -free NaOH solutions and determining the equivalence point by Gran's method^{54,55} that determines the standard potential, E_0 , and the liquid junction potential, j . The phosphorus concentration in the ligand stock solution was determined colorimetrically with a Mo(V)–Mo(VI) reagent.⁵⁸ These calibrations of the glass electrode were performed under almost the same condition of ionic strength as the titrations for the protonation constants. All titrations were carried out at least 3 times, and all titrations showed good agreement with each other. After the titrations, the ^{31}P NMR spectra of the sample solutions was measured as described in Section 2.2, and there was no change which showed the decomposition of the sample. The nonlinear least squares curve fitting by Levenberg–Marquardt algorithm for the determination of the protonation constants were carried out by KaleidaGraph 4.1 (Synergy Software).

2.3. ^{31}P NMR measurements

First protonation constants of $\text{cP}_4\text{O}_{12-n}(\text{NH})_n^{4-}$ ($n = 0, 2, 3, 4$) anions were also determined by ^{31}P NMR measurements. All NMR spectra were recorded by a Bruker DPX-250 (5.87T) superconducting Fourier-transform pulse NMR spectrometer with a 10 mm tunable broad-band probe

which was operated at 101.258 MHz and 25.0 ± 1.0 °C. The temperature of the sample solution was calibrated by 1,2-ethanediol with Van Geet's method.^{59,60} An acquisition time was 2.0 s, and the FID were collected in 100000 data points, and was used a sweep width of 25 kHz, that is, the digital resolution in the frequency dimension was 0.5 Hz (0.0049 ppm). In order to avoid saturation of the resonances, the intervals between each FID scan were 5.0 s or over.⁶¹ The NMR chemical shifts were recorded against an external standard of 75% H₃PO₄ in 10% D₂O. In the case of the determination of the protonation constants, the spectrometer was not field frequency locked during the measurement of the sample solutions, because D₂O was not added in order to retain the solvent purity, and it was confirmed that the chemical shift of the reference solution hardly varied before and after a series of NMR measurement. All spectra were recorded in the absence of ¹H decoupling. A 3 mL quantity of 0.01 mol·L⁻¹ Na₄cP₄O_{12-n}(NH)_n (*n* = 0, 3, 4) + 0.1 mol·L⁻¹ NaNO₃ added to an NMR tube of 10 mm in outside diameter, and small aliquots of HNO₃ or NaOH aqueous solution which contains 0.1 mol·L⁻¹ NaNO₃ was added by a micro syringe in order to define the pH of the solutions, hence all ³¹P NMR measurements were performed under the constant ionic strength. The pH meter readings were recorded just before the ³¹P NMR measurements, and were carried out by an Orion 250A pH meter with a Horiba 6069-10C micro glass electrode. The micro glass electrode was calibrated at pH 4, 7 and 9 with a phthalate buffer, a phosphate buffer, and a tetraborate buffer, respectively. All ³¹P NMR measurements were carried out 3 times, and the measurements showed good agreement with each other. The nonlinear least squares curve fitting by Levenberg–Marquardt algorithm for the determination of the protonation constants and the intrinsic ³¹P NMR chemical shifts were carried out by KaleidaGraph 4.1 (Synergy Software).

2.4. Observation of thermal decomposition behavior

Thermo-gravimetric (TG) analysis and differential thermal analysis (DTA) measurements were committed from ambient temperature to 500 °C at a heating rate of 10 °C·min⁻¹ in an air atmosphere using Thermo Plus 8120 (Rigaku Co. Ltd.). 20.0 mg Na₄cP₄O_{12-n}(NH)_n (*n* = 3, 4) were put in a platinum crucible (I.D. 5.0 mm, depth 2.5 mm) and 20.0 mg of calcined α-Al₂O₃ powder was used as reference for each measurement. The crystalline structures of Na₄cP₄O_{12-n}(NH)_n (*n* = 3, 4), were investigated using an X-ray diffractometer (XRD; Rigaku RINT 1200M) equipped with a scintillation detector, and a rotating Cu anode operating radiation at 40 kV and 40 mA. The 2θ/θ scans were carried out, and a scan rate of 3° per minute was applied within the range of 5–60°.

3. Results and discussion

3.1. Optimization of synthesis condition and pH-controlled recrystallization of Na₄cP₄O₉(NH)₃.

H₂O

In the hydrolysis reaction of the cyclic imidopolyphosphate, the continuous processes in three stages is already clear, namely, (i)the cleaving of the cyclic molecular skeleton, (ii)the substitution reaction to an oxygen atom of an imino group, and (iii)the ring closure reaction.^{62,63} Specifically, Na₄cP₄O₉(NH)₃ is synthesized by the hydrolysis of Na₄cP₄O₈(NH)₄ as the starting material under acidic condition. The cleaving of the cyclic molecular skeleton in the first stage hardly proceeds when the acid is too weak. Not only imino group but also phosphate group eliminate in the second stage when the acid is too strong,⁵² as a result, the generation of the Na₃cP₃O₆(NH)₃ is brought about. Therefore, the careful selection of the weak acid and the close examination of its concentration are indispensable for the hydrolysis reaction of Na₄cP₄O₈(NH)₄. Table S1 shows the reaction products by the hydrolysis reaction of Na₄cP₄O₈(NH)₄, under various reaction conditions including several types of acids and alkalis and their concentrations, various solvents, the reaction temperature, and the reaction time. Na₄cP₄O₈(NH)₄ was barely hydrolyzed in alkaline aqueous solutions and organic solvents. In inorganic and organic

acids whose pK_1 (the first acid dissociation constant) was less than 4, $\text{Na}_3\text{cP}_3\text{O}_{(9-n)}(\text{NH})_n$ ($n = 1, 2$) as six-membered compounds were generated, and in inorganic acids whose pK_1 was less than 2, the ring structure cleaved and $\text{Na}_5\text{P}_3\text{O}_{10}$ as a short-chain phosphate was generated. After all it clarified that propionic acid was the most suitable for the synthesis of $\text{Na}_4\text{cP}_4\text{O}_9(\text{NH})_3$, hence 6 g of $\text{Na}_4\text{cP}_4\text{O}_8(\text{NH})_4 \cdot 2\text{H}_2\text{O}$ was dissolved in 300 mL of 0.2 mol L^{-1} propionic acid as a relatively weak organic acid, and hydrolyzed in an oil bath at $80 \text{ }^\circ\text{C}$ for 8 hours. After cooling to room temperature, the reaction solution was neutralized by NaOH and 150 mL of acetone was added. The reaction solution was suction filtered to remove unreacted starting material and the by-product $\text{Na}_3\text{cP}_3\text{O}_{(9-n)}(\text{NH})_n$ ($n = 0-2$). A large excess amount of acetone was added to the filtrate, then the precipitate was suction filtered and washed with 25 mL of ethanol followed by 50 mL of acetone. The precipitate was vacuum dried, and 6.6 g of white product was obtained containing about 2% $\text{Na}_4\text{cP}_4\text{O}_9(\text{NH})_3 \cdot x\text{H}_2\text{O}$ with one of the four imino groups replaced by an oxygen atom. The synthesis procedure of $\text{Na}_4\text{cP}_4\text{O}_9(\text{NH})_3 \cdot x\text{H}_2\text{O}$ as mentioned above is illustrated in Scheme 2. Fig. 1(top) shows the ^{31}P NMR spectrum of this raw product.

In the case of most conventional recrystallization, a pure substance and impurities are separated using the difference in solubilities which were based on the temperature of a solution or the composition of a solvent. However, the product $\text{Na}_4\text{cP}_4\text{O}_9(\text{NH})_3 \cdot x\text{H}_2\text{O}$ and the starting material $\text{Na}_4\text{cP}_4\text{O}_8(\text{NH})_4 \cdot 2\text{H}_2\text{O}$ have similar molecular structures, as well as similar physical and chemical properties, and are difficult to separate by conventional recrystallization. Therefore, in this study, the raw product was purified by a pH-controlled recrystallization process applying the difference in the basicities of $\text{Na}_4\text{cP}_4\text{O}_9(\text{NH})_3 \cdot x\text{H}_2\text{O}$ and $\text{Na}_4\text{cP}_4\text{O}_8(\text{NH})_4 \cdot 2\text{H}_2\text{O}$ as illustrated in Scheme 3. The basicities of a series of *cyclo*- μ -imidotriphosphate anions, $\text{cP}_3\text{O}_{9-n}(\text{NH})_n^{3-}$ ($n = 0-3$) have been reported to increase in proportion to the number of imino groups in the molecule.^{36,42} Assuming that this regularity holds for a series of *cyclo*- μ -imidotetraphosphate anions, $\text{cP}_4\text{O}_{(12-n)}(\text{NH})_n^{4-}$ ($n = 0-4$), we estimated the

pK_1 of $cP_4O_9(NH)_3^{4-}$ to be ca. 3.2, thus the raw product was dissolved in a small amount of water and adjusted to pH 2.5 by nitric acid. At this pH, almost all of the $cP_4O_8(NH)_4^{4-}$ was protonated, on the other hand, about 35% of the $cP_4O_9(NH)_3^{4-}$ would remain dissociated. The water solubility of the protonated anion decreases due to the decrease in negative charges.^{64–66} Therefore, 75 vol% of acetone was added to this solution, and the starting material $Na_4cP_4O_8(NH)_4$ precipitated. The precipitate was removed by suction filtration. A large excess amount of acetone was added to the filtrate and a white precipitate was collected by suction filtration, then washed with 5 mL of ethanol followed by 10 mL of acetone. Against the past reports by other researchers,^{43,52,62,63,67–70} acetone is more suitable for the final washing than alcohol for the syntheses of various inorganic phosphates. Since acetone do not readily form hydrogen bonds with inorganic phosphates, the powder is prevented being strongly adhered mutually, and kept to a better powdery state. The precipitate was vacuum dried, and 0.42 g of white product was obtained containing about 20% $Na_4cP_4O_9(NH)_3 \cdot xH_2O$. The above pH-controlled recrystallization was performed again and the purity of $Na_4cP_4O_9(NH)_3 \cdot xH_2O$ increased to 95%, and the overall yield was 0.11 g, 1.9%. Elem. Anal. Found: Na, 21.47; P, 29.21; O, 33.90; NH, 10.83; H_2O , 4.59. Requires: Na, 21.74; P, 29.30; O, 34.05; NH, 10.65; H_2O , 4.26. $Na_4cP_4O_9(NH)_3$ was characterized as a monohydrate by the elementary analysis.

Fig. 1(bottom) shows the ^{31}P NMR spectrum of $Na_4cP_4O_9(NH)_3 \cdot H_2O$ after the pH-controlled recrystallizations of two times. The $cP_4O_9(NH)_3$ molecule contains two types of magnetically non-equivalent phosphorus nuclei, i.e., two nuclei in $-NH-PO_2-NH-$ and two nuclei in $-O-PO_2-NH-$ as shown in Fig. 1, therefore, two pairs of doublets were observed at -1.5 and -7.9 ppm. These values are in close agreement with the intrinsic chemical shifts of the phosphorus nuclei of $-NH-PO_2-NH-$ in $cP_3O_6(NH)_3^{3-}$ anion, i.e., 1.5 ppm,³⁹ and that of $-O-PO_2-NH-$ in $cP_3O_7(NH)_2^{3-}$ anion, i.e., -8.5 ppm,³⁶ have been previously reported. The value of the $^2J(^{31}P-^{31}P)$ coupling constant is 3.9 Hz, which is relatively small. This is probably because the molecular structure of $cP_4O_9(NH)_3$ molecule is distorted due to two different bridging atoms.⁷¹ A slight singlet resonance was observed at -8.8 ppm. All of the

phosphorus nuclei in the molecule which is the origin of this singlet resonance are magnetically equivalent. In addition, the chemical shift of the singlet resonance is in agreement with the intrinsic chemical shifts of the phosphorus nuclei of $-\text{O}-\text{PO}_2-\text{NH}-$ in $\text{cP}_3\text{O}_7(\text{NH})_2^{3-}$ anion (-8.5 ppm^{36}) and in $\text{cP}_4\text{O}_9(\text{NH})_3^{4-}$ (-7.9 ppm) anion. This suggests that the singlet resonance arises from *trans*- $\text{cP}_4\text{O}_{10}(\text{NH})_2$ molecule. This assignment of the ^{31}P NMR signal to *trans*- $\text{cP}_4\text{O}_{10}(\text{NH})_2$ molecule is strongly confirmed by the protonation constant determined from the pH titration profile of the chemical shift of the signal and the "independent site model" for the protonation equilibria as discussed in the following section. In the present study, the isolation and purification of *trans*- $\text{Na}_4\text{cP}_4\text{O}_{10}(\text{NH})_2$ could not be achieved because only a trace amount of the ligand was produced. However, it will be synthesized in the near future.

3.2. Protonation and lactam-lactim tautomerism equilibria

Protonation equilibria for $\text{cP}_4\text{O}_{12-n}(\text{NH})_n^{4-}$ ($n = 0, 3, 4$) can be represented as follows:



Thus the protonation constants of $\text{cP}_4\text{O}_{12-n}(\text{NH})_n^{4-}$ ($n = 0, 3, 4$), K_{H} , are defined as follows:

$$K_{\text{H}} = \frac{[\text{HL}^{3-}]}{[\text{H}^+][\text{L}^{4-}]} \quad (2)$$

On the other hand, the average number of bound H^+ ions per ligand molecule, \bar{n} , can be calculated by dividing the concentrations of bound H^+ ions, $[\text{H}^+]_{\text{b}}$, by the total concentration of ligand ions, C_{L} .

Because $[\text{H}^+]_b$ is given as the difference of the total concentration of H^+ ions, C_H , and the free H^+ ion concentration of the equilibrium solution, $[\text{H}^+]$, \bar{n} can be determined as:

$$\bar{n} = \frac{[\text{H}^+]_b}{C_L} = \frac{(C_H - [\text{H}^+])}{C_L} \quad (3)$$

Using eqn (2), \bar{n} can also be expressed as:

$$\bar{n} = \frac{K_H[\text{H}^+]}{1 + K_H[\text{H}^+]} \quad (4)$$

The \bar{n} versus $\log [\text{H}^+]$ plots obtained for $\text{cP}_4\text{O}_{12-n}(\text{NH})_n^{4-}$ ($n = 0, 3, 4$) are shown in Fig. 2. The $\log K_H$ values at 25.0 ± 0.5 °C and $I = 0.10$ (NaNO_3) that minimize the error-square sum of chemical shifts, $\Sigma(\bar{n}_{\text{obs}} - \bar{n}_{\text{calc}})^2$, were calculated using a nonlinear least squares curve fitting method as listed in Table 1. The solid lines in Fig. 2 are calculated from the appropriate $\log K_H$ values, and show good agreement with the experimental results. The determination of the $\log K_H$ values for the repetition titration at least three times was carried out, and all $\log K_H$ values showed good agreement with each other.

As reported by our previous work, the stepwise protonation constants of the series of thiomonophosphate anions, $\text{PO}_{4-n}\text{S}_n^{3-}$ ($n = 0-4$), decrease with an increase in the number of sulfur atoms neighboring the central phosphorus atom.⁷² On the other hand, the first protonation constants of the $\text{cP}_3\text{O}_{9-n}(\text{NH})_n^{3-}$ ($n = 0-3$) increase approximately linearly with an increase in the number of imino groups that constitute the ligand molecules as can be seen in Table S2. It should be pointed that the $\log K_H$ values of the $\text{cP}_4\text{O}_{12-n}(\text{NH})_n^{4-}$ ($n = 0, 3, 4$) increase with an increase in the number of imino groups, n , as well as $\text{cP}_3\text{O}_{9-n}(\text{NH})_n^{3-}$ ($n = 0-3$), showing that the basicity of the phosphate groups in the cyclic

tetramers increases with the replacement of P–O–P linkages by P–NH–P linkages of the ligand molecules.^{36,42} Since the electronegativity of nitrogen atom is smaller than that of oxygen atom and the electron density around the central phosphorus atom of the phosphate unit containing imino group(s) is expected to be higher than that of the PO₄ tetrahedral units, it is anticipated that H⁺ ions bind more preferentially to the phosphate groups in the order of O–P–O < NH–P–O < NH–P–NH.

The NMR measurements can give precise and microscopic information on the nature of the protonation equilibria and a tautomerism behavior.^{73–78} The outstanding informative merit of NMR reveals itself in providing quantitative information on an equilibrium system, i.e., determination of protonation constants as well as in providing an information on a molecular structure.^{79,80} Furthermore, the isolation of *trans*–Na₄cP₄O₁₀(NH)₂ was impossible because of extremely little yield as can be seen in Fig. 1(bottom), however the protonation constant of *trans*–cP₄O₁₀(NH)₂^{4–} can be determined without any previous purification, because the NMR signals corresponding to cP₄O_{12–n}(NH)_n^{4–} (*n* = 2, 3, 4) are well resolved.⁷² The pH titration profiles of the ³¹P NMR chemical shifts of the phosphorus atoms belonging to cP₄O_{12–n}(NH)_n^{4–} (*n* = 0, 2, 3, 4) are shown in Fig. 3. The pH dependence of the chemical shifts can be interpreted in terms of the protonation of these anions. In spite of the presence of protonated and non protonated species, only sharp singlet resonances are observed in the ³¹P NMR spectra over the entire pH range for each anion. This indicates that the proton exchanges of these anions are much faster than the NMR time scale.⁸¹ Therefore, the ³¹P NMR chemical shifts of the phosphorus nuclei belonging to the protonated and non-protonated species of each anion are averaged by fast exchange over both species that are present in eqn (1), and can be written as:⁸²

$$\delta_{\text{P}} = \frac{\delta_{\text{L}^{4-}} [\text{L}^{4-}] + \delta_{\text{HL}^{3-}} [\text{HL}^{3-}]}{C_{\text{L}}} \quad (\text{L} = \text{cP}_4\text{O}_{12-n}(\text{NH})_n \quad (n = 0, 2, 3, 4)) \quad (5)$$

where C_L is the total concentration of the ligand in solution, δ_p is the observed ^{31}P NMR chemical shift, and $\delta_{L^{4-}}$ and $\delta_{HL^{3-}}$ refer to the intrinsic ^{31}P NMR chemical shifts of the phosphorus nuclei belonging to each species. Using the mass action law for this system of equilibria as eqn (2), the observed chemical shift can be expressed as:⁸²

$$\delta_p = \frac{\delta_{L^{4-}} + K_H [H^+] \delta_{HL^{3-}}}{1 + K_H [H^+] \delta_{HL^{3-}}} \quad (6)$$

The $\log K_H$ values and the intrinsic chemical shift of each species have been determined by the nonlinear least squares curve fitting method with the plots of δ_p versus pH (Fig. 3) as listed in Table 2. The solid lines in Fig. 3 are calculated curves obtained by using the pertinent values from Table 2 and show good agreement with the experimental results, and the determination of these values for the repetition experiment at least three times was carried out, and all values showed good agreement with each other. It should be noted that the $\log K_H$ values determined by the ^{31}P NMR and potentiometric titration methods were almost within experimental error of one another, despite the difference in principles of the two methods. This indicates the validity of the protonation constants as well as the intrinsic shift values evaluated by the present study.

A good proportionality is established between the $\log K_H$ of $\text{cP}_4\text{O}_{12-n}(\text{NH})_n^{4-}$ ($n = 0, 2, 3, 4$) and the number of imino groups which constitute the ligand molecules as well as the protonation equilibria of $\text{cP}_3\text{O}_{9-n}(\text{NH})_n^{3-}$ ($n = 0-3$) which has already been reported⁴² as can be seen Fig. 4. In order to understand more precisely the increment of the macroscopic protonation constant with the number of imino groups of the $\text{cP}_4\text{O}_{12-n}(\text{NH})_n^{4-}$ and $\text{cP}_3\text{O}_{9-n}(\text{NH})_n^{3-}$, it is assumed that the macroscopic protonation reactions can be divided into three microscopic protonation processes at the non-bridging

oxygen atoms of the phosphate groups, i.e., $\log K_H$ can be expressed in the following additive form of independent microscopic protonation constants, $\log k_H$, at three phosphate sites,

$$\log K_H = i \cdot \log k_H(\text{O,O}) + j \cdot \log k_H(\text{O,N}) + k \cdot \log k_H(\text{N,N}) \quad (7)$$

where $\log k_H(\text{O,O})$, $\log k_H(\text{O,N})$, and $\log k_H(\text{N,N})$ indicate the microscopic protonation constants for O–P–O, O–P–NH, and NH–P–NH groups, respectively, and i , j , and k stand for the numbers of the respective phosphate groups in the $\text{cP}_4\text{O}_{12-n}(\text{NH})_n$ and $\text{cP}_3\text{O}_{9-n}(\text{NH})_n$ molecules. The $\log k_H(\text{O,O})$ value can be calculated from the macroscopic protonation constant of $\text{cP}_4\text{O}_{12}^{4-}$ which consists of only O–P–O group, i.e., $1.79 / 4 = 0.45$. In the same way, $\log k_H(\text{O,N})$ and $\log k_H(\text{N,N})$ values can be calculated from the $\log K_H$ of *trans*- $\text{cP}_4\text{O}_{10}(\text{NH})_2^{4-}$ and $\text{cP}_4\text{O}_8(\text{NH})_4^{4-}$ which consist of only O–P–NH and NH–P–NH groups, respectively, i.e., $2.59 / 4 = 0.65$ and $3.73 / 4 = 0.93$. The calculated $\log K_H$ of $\text{cP}_4\text{O}_9(\text{NH})_3^{4-}$ using the $\log k_H(\text{O,N})$ and $\log k_H(\text{N,N})$ values, i.e., $0.65 \times 2 + 0.93 \times 2 = 3.16$, is good agreement with the experimental value 3.09. The establishment of the independent site model as mentioned above suggests the validity for the ^{31}P NMR signal assignment and the determination of $\log K_H$ value by the pH titration profiles of the ^{31}P NMR chemical shift for *trans*- $\text{cP}_4\text{O}_{10}(\text{NH})_2^{4-}$. In addition, the $\log K_H$ of $\text{cP}_3\text{O}_{9-n}(\text{NH})_n^{3-}$ ($n = 0-3$) can be also the microscopic protonation constants as listed in Table S2 together with the experimental values. The experimental data and the calculated values show almost agreement with each other, and it suggests that a macroscopic protonation constants of a series of *cyclo*-polyphosphate and *cyclo*- μ -imidopolyphosphate anions can be expressed by the linear combination of a microscopic protonation constants as eqn (7). In the independent site model, there are two points which should be noted. In the first place, the experimental $\log K_H$ of $\text{cP}_3\text{O}_{9-n}(\text{NH})_n$ ($n = 0, 1$) are smaller than the calculated $\log K_H$ of the corresponding anions, whereas the experimental $\log K_H$ of $\text{cP}_3\text{O}_{9-n}(\text{NH})_n$ ($n = 2, 3$) are larger than the calculated $\log K_H$ of the corresponding anions. In

the next place, for $\text{cP}_4\text{O}_{12-n}(\text{NH})_n^{4-}$ ($n = 0, 2, 4$) anions, the difference between the $\log k_{\text{H}}(\text{N},\text{N})$ and the $\log k_{\text{H}}(\text{O},\text{N})$ values, i.e., $0.93 - 0.65 = 0.28$, is larger than the difference between the $\log k_{\text{H}}(\text{O},\text{N})$ and the $\log k_{\text{H}}(\text{O},\text{O})$ values, i.e., $0.65 - 0.45 = 0.20$. This affinity to proton of $\text{NH}-\text{P}-\text{NH}$ group leads us to consider an important aspect in the protonation of a series of *cyclo*- μ -imidopolyphosphate anions, i.e., lactam-lactim tautomerism⁸³⁻⁸⁷ of imino phosphate group as shown in Scheme 4. Tautomerism is the existence of two or more molecular structures, i.e., tautomers, which are capable of facile interconversion (in many cases merely exchanging a hydrogen atom between two other hetero atoms) of which it forms a covalent bond.⁸⁸ In general, because the activation energy of the exchange reaction between tautomers is relatively slight, the exchange rate of the tautomerism is extremely fast. Hence the tautomerism can be considered to be the intramolecular hydrogen bonding between hetero atoms (bridging nitrogen atoms and non-bridging oxygen atoms in the case of the imidophosphate anions) in the longer time scale. Therefore, the neighboring imino phosphate units linked by the $\text{P}-\text{NH}-\text{P}$ bonding should be affected each other through this lactam-lactim tautomerism. It can be estimated that the stabilization of the protonated species by such an intramolecular hydrogen bonding becomes driving force of the enhancement of the protonation of the ligands. Delocalization of H^+ ions, through the tautomerism, on the whole ring molecule of $\text{cP}_3\text{O}_6(\text{NH})_3$ and $\text{cP}_4\text{O}_8(\text{NH})_4$, for example, is expected to enhance the protonation. In conclusion, the increase in the $\log K_{\text{H}}$ with an increase in the number of imino groups is not only due to the basicity of the imino group, but also due to the lactam-lactim tautomerism between the phosphate units linked by the $\text{P}-\text{NH}-\text{P}$ bonding.

The ^{31}P NMR chemical shift changes induced by the protonation of $\text{cP}_4\text{O}_{12-n}(\text{NH})_n^{4-}$ ($n = 0, 4$) are smaller than that of $\text{cP}_4\text{O}_{12-n}(\text{NH})_n^{4-}$ ($n = 2, 3$) as shown in Fig. 3. Because the $\text{cP}_4\text{O}_{12-n}(\text{NH})_n^{4-}$ ($n = 0, 4$) contain only unity kind of coordination atoms, these anions have symmetric molecular structure. Thus, the $\text{O}-\text{P}-\text{O}$ and $\text{NH}-\text{P}-\text{NH}$ bond angles of the both anions are almost changeless by protonation, so the nuclear screenings of the central phosphorus atoms of these anions do not change all over the pH

range.⁷² It is notable that the $\log K_H$ values evaluated by the δ_p versus pH profiles (Table 2) of $-\text{O}-\text{PO}_2-\text{NH}-$ and $-\text{NH}-\text{PO}_2-\text{NH}-$ phosphorus atoms belonging to $\text{cP}_4\text{O}_9(\text{NH})_3^{4-}$ are consistent with each other within the experimental error, i.e., 3.11 and 3.07. This indicates the protonation is not independent of the respective phosphate groups. The concurrent change observed in the shift values of the $-\text{O}-\text{PO}_2-\text{NH}-$ and $-\text{NH}-\text{PO}_2-\text{NH}-$ phosphorus nuclei of $\text{cP}_4\text{O}_9(\text{NH})_3^{4-}$ can reasonably be explained by the lactam-lactim tautomerism as mentioned above, i.e., the protonation equilibrium of imino groups can be represented as Scheme 5. Since the intrinsic chemical shift values of respective phosphorus nuclei have been determined as can be seen in Table 2, it is of interest to relate the intrinsic chemical shift values of the central phosphorus nuclei for $-\text{O}-\text{PO}_2-\text{O}-$, $-\text{O}-\text{PO}_2-\text{NH}-$, and $-\text{NH}-\text{PO}_2-\text{NH}-$ linkages determined by the present study with the numbers of oxygen and/or nitrogen atoms bonded to the central phosphorus atoms, because an additivity rule has already been reported on phosphorus-nitrogen compounds.⁸⁹ The intrinsic chemical shift values of the central phosphorus nuclei of the deprotonated $\text{cP}_4\text{O}_{12-n}(\text{NH})_n^{4-}$ ($n = 0, 2, 3, 4$) can empirically be expressed as in an additive form as,

$$\delta_L^{\text{cal}} = n_{\text{O}} \cdot \delta_L^{\text{O}} + n_{\text{N}} \cdot \delta_L^{\text{N}} \quad (8)$$

where δ_L^{cal} indicates the calculated intrinsic chemical shift value; n_{O} and n_{N} stand for the numbers of the bridging oxygen and nitrogen atoms in the phosphate unit, and δ_L^{O} and δ_L^{N} represent the contribution of the respective bridging atoms. The δ_L^{O} and δ_L^{N} values can be estimated as the half δ_L values of $\text{cP}_4\text{O}_{12-n}(\text{NH})_n^{4-}$ ($n = 0, 4$) which consists of only unity kind of coordination atoms, respectively, i.e., $\delta_L^{\text{O}} = -20.43/2 = -10.22$ (ppm) and $\delta_L^{\text{N}} = -0.61/2 = -0.31$ (ppm). The experimental intrinsic chemical shifts as listed in Table 2, δ_L^{exp} , are plotted against the δ_L^{cal} values calculated by eqn

(8) as shown in Fig. 5. Even though it is obvious that the δ_L^{exp} values can be expressed by eqn (8), the small deviations due to the effect of the third bridging atoms in the cyclic molecules cannot be ignored. Namely, the δ_L^{exp} value for $-\text{O}-\text{PO}_2-\text{NH}-$ linkage of *trans*- $\text{cP}_4\text{O}_{10}(\text{NH})_2^{4-}$ shift to higher magnetic field than that of $\text{cP}_4\text{O}_9(\text{NH})_3^{4-}$. This additivity rule can also be applicable to the interpretation of the ^{31}P NMR chemical shift values of respective phosphorus nuclei belonging to the protonated anions. In this case, the calculated shift values, $\delta_{\text{HL}}^{\text{cal}}$, can be expressed as,

$$\delta_{\text{HL}}^{\text{cal}} = n_{\text{O}} \cdot \delta_{\text{HL}}^{\text{O}} + n_{\text{N}} \cdot \delta_{\text{HL}}^{\text{N}} \quad (9)$$

In Fig. 5 are also plotted the $\delta_{\text{HL}}^{\text{obs}}$ values against the $\delta_{\text{HL}}^{\text{cal}}$ values calculated by use of $\delta_{\text{HL}}^{\text{O}} = -10.30$ (ppm) and $\delta_{\text{HL}}^{\text{N}} = 0.005$ (ppm), respectively. A comparison of the plots between the δ_L^{obs} versus the δ_L^{cal} and the $\delta_{\text{HL}}^{\text{obs}}$ versus the $\delta_{\text{HL}}^{\text{cal}}$ indicates a better linearity for the $\delta_{\text{HL}}^{\text{obs}}$ versus the $\delta_{\text{HL}}^{\text{cal}}$ relationships. Consistency in the respective magnetic environments of $-\text{O}-\text{PO}_2-\text{O}-$, $-\text{O}-\text{PO}_2-\text{NH}-$, and $-\text{NH}-\text{PO}_2-\text{NH}-$ phosphorus nuclei belonging to different protonated anions indicate that the effect of proton binding on the four phosphorus groups of protonated anions is equivalent. The delocalization of protons which is caused by the lactam-lactim tautomerism on the whole ring molecule of $\text{cP}_4\text{O}_{12-n}(\text{NH})_n^{4-}$ can explain this additivity rule for the ^{31}P NMR intrinsic chemical shift as well as the independent site model for macroscopic protonation equilibria as eqn (7) and the remarkable proton affinity of $\text{NH}-\text{P}-\text{NH}$ group as mentioned above. The delocalization of the dissociatable proton on the whole ring molecule suggests the possibility as the proton conductor of all *cyclo*- μ -imidophosphates.^{90,91}

3.3. Thermal decomposition behavior of $\text{Na}_4\text{cP}_4\text{O}_9(\text{NH})_3 \cdot \text{H}_2\text{O}$

Fig. 6 shows TG-DTA curves of $\text{Na}_4\text{cP}_4\text{O}_9 \cdot 4\text{H}_2\text{O}$, $\text{Na}_4\text{cP}_4\text{O}_9(\text{NH})_3 \cdot \text{H}_2\text{O}$ and $\text{Na}_4\text{cP}_4\text{O}_8(\text{NH})_4 \cdot 2\text{H}_2\text{O}$ heated to 500 °C. In all phosphates, there are two endothermic peaks at about 100 and 200 °C accompanied by a rapid weight loss. These thermal processes are caused by the removal of the adsorbed water at 100 °C and of the crystallization water at 200 °C. $\text{Na}_4\text{cP}_4\text{O}_9(\text{NH})_3$ was reconfirmed as a monohydrate from weight loss due to the desorption of crystallization water. It should be noted that in $\text{Na}_4\text{cP}_4\text{O}_9(\text{NH})_3 \cdot \text{H}_2\text{O}$, two exothermic peaks due to the pyrolytic elimination of imino groups were observed at 240 and 290 °C. This suggests the pyrolytic elimination of the imino groups in two-stage. In both the $\text{cP}_3\text{O}_{(9-n)}(\text{NH})_n^{3-}$ ($n = 0-3$) which have been reported^{62,63} and $\text{cP}_4\text{O}_{12-n}(\text{NH})_n^{4-}$ ($n = 0, 4$) anions, the pyrolytic elimination of imino groups was completed in a single step. On the other hand, two types of imino groups with mutually dissimilar chemical environments are present in the $\text{Na}_4\text{cP}_4\text{O}_9(\text{NH})_3$ molecule. In other words, when we pay attention to the bridging atoms *except phosphorus atoms*, the following characteristics are noted: (1) an imino group ($-\text{O}-\text{PO}_2-\text{NH}-\text{PO}_2-\text{NH}-$) adjacent to one bridging nitrogen atom and (2) an imino group ($-\text{NH}-\text{PO}_2-\text{NH}-\text{PO}_2-\text{NH}-$) adjacent to two nitrogen bridging atoms are present in the *cyclo-tri- μ -imidotetraphosphate* anions, namely, this is probably the reason for the pyrolytic elimination of the imino groups in two-stage. These findings suggest the possibility that during combustion, $\text{Na}_4\text{cP}_4\text{O}_9(\text{NH})_3 \cdot \text{H}_2\text{O}$ exhibits a flame retardant effect over a wide range of temperatures. Furthermore, pyrolytic elimination of $\text{Na}_4\text{cP}_4\text{O}_9(\text{NH})_3 \cdot \text{H}_2\text{O}$ in the first step occurs at the relatively low temperature of around 240 °C, indicating that the flame retardant effect is exhibited in the initial stage of combustion. Fig. 7 shows the XRD analysis of $\text{Na}_4\text{cP}_4\text{O}_9(\text{NH})_3 \cdot \text{H}_2\text{O}$ and $\text{Na}_4\text{cP}_4\text{O}_8(\text{NH})_4 \cdot 2\text{H}_2\text{O}$. $\text{Na}_4\text{cP}_4\text{O}_9(\text{NH})_3 \cdot \text{H}_2\text{O}$ presents an amorphous structure. $\text{Na}_4\text{cP}_4\text{O}_9(\text{NH})_3$ has asymmetrical molecular structure, hence the number of arrangement patterns in realignment of the molecule will increase. As a result, when the pH-controlled recrystallization, it is presumed that the long-distance order decreases and $\text{Na}_4\text{cP}_4\text{O}_9(\text{NH})_3$ shows an amorphous structure. The XRD patterns at 350 °C show that after the pyrolytic elimination of the imino groups, the

molecular structure of both compounds changed to $\text{Na}_3\text{cP}_3\text{O}_9$. The XRD patterns at 250 °C show that $\text{Na}_4\text{cP}_4\text{O}_8(\text{NH})_4 \cdot 2\text{H}_2\text{O}$ has been changed into nonhydrate and the imino groups are hardly pyrolytically eliminated, meanwhile, in $\text{Na}_4\text{cP}_4\text{O}_9(\text{NH})_3 \cdot \text{H}_2\text{O}$, the pyrolytic elimination of the imino groups and the generation of $\text{Na}_4\text{cP}_4\text{O}_{12}$ have already been brought about. Pyrolytic elimination in two-stage over a wide range of temperatures is therefore also suggested by the results of the XRD analysis.

4. Conclusions

$\text{Na}_4\text{cP}_4\text{O}_9(\text{NH})_3 \cdot \text{H}_2\text{O}$ was synthesized by the hydrolysis of $\text{Na}_4\text{cP}_4\text{O}_8(\text{NH})_4 \cdot 2\text{H}_2\text{O}$ in 0.2 mol L⁻¹ propionic acid as a very weak acid and isolated by the pH-controlled recrystallization. The first protonation constants and the intrinsic ³¹P NMR chemical shifts of each protonated species of $\text{cP}_4\text{O}_{12-n}(\text{NH})_n^{4-}$ ($n = 0, 2, 3, 4$) anions were determined. The basicities of these anions increase linearly with an increase in the number of imino groups in the anions as well as $\text{cP}_3\text{O}_{9-n}(\text{NH})_n^{3-}$ ($n = 0-3$) anions. Macroscopic protonation constants can be expressed in the additive form of the independent microscopic protonation constants for three phosphate sites, i.e., $-\text{O}-\text{PO}_2-\text{O}-$, $-\text{O}-\text{PO}_2-\text{NH}-$, and $-\text{NH}-\text{PO}_2-\text{NH}-$ groups. The neighboring imino phosphate units linked by the P-NH-P bonding were affected each other through the lactam-lactim tautomerism, therefore the $-\text{NH}-\text{PO}_2-\text{NH}-$ group shows especially high basicity. The lactam-lactim tautomerism on the whole ring molecule of $\text{cP}_4\text{O}_{12-n}(\text{NH})_n^{4-}$ could explain the additivity rule of the ³¹P NMR intrinsic chemical shift and the independent site model for macroscopic protonation equilibria. The delocalization of the dissociatable proton on the whole ring molecule which occurred by the lactam-lactim tautomerism suggests the possibility as the proton conductor of various *cyclo*-μ-imidophosphates. TG-DTA result showed a two-stage pyrolytic elimination of imino groups over a wide range of temperatures from $\text{Na}_4\text{cP}_4\text{O}_9(\text{NH})_3 \cdot \text{H}_2\text{O}$ molecule, moreover, the first step pyrolytic elimination of imino groups occurred at lower temperature than the case of $\text{Na}_4\text{cP}_4\text{O}_8(\text{NH})_4 \cdot 2\text{H}_2\text{O}$, i.e., 240 °C. XRD result showed that the generation of $\text{Na}_4\text{cP}_4\text{O}_{12}$ have

been brought about before the thermal decomposition into $\text{Na}_3\text{CP}_3\text{O}_9$. These results show that the flame retardant effect is exhibited from the initial stage of combustion over a wide temperature range.

Acknowledgements

This study was supported by the Japan Society for the Promotion of Science (JSPS) KAKENHI Grant-in-Aid for Young Scientists (B) (No. 16750133).

References

- 1 Y. Wang, Y. Li, F. Liu, Y. Li, L. Song, H. Li, C. Meng and J. Wu, *Agr. Ecosyst. Environ.*, 2014, **184**, 9.
- 2 W. Guo, Y. Fu, B. Ruan, H. Ge and N. Zhao, *Ecol. Indic.*, 2014, **36**, 254.
- 3 X. Yan, D. Wang, H. Zhang, G. Zhang and Z. wei, *Agr. Ecosyst. Environ.*, 2013, **175**, 47.
- 4 D. A. Bell, B. F. Towler and M. Fan, *Coal Gasification and Its Applications*, William Andrew, New York, 1st edn, 2011, Chap. 11.
- 5 S. Fei and H. R. Allcock, *J. Power Sources*, 2010, **195**, 2082.
- 6 Y. J. Shin, Y. R. Ham, S. H. Kim, D. H. Lee, S. B. Kim, C. S. Park, Y. M. Yoo, J. G. Kim, S. H. Kwon and J. S. Shin, *J. Ind. Eng. Chem.*, 2010, **16**, 364.
- 7 B. Çoşut, F. Hacivelioglu, M. Durmuş, A. Kılıç and S. Yeşilot, *Polyhedron*, 2009, **28**, 2510.
- 8 M. Gleria, R. Bertani, R. D. Jaeger and S. Lora, *J. Fluorine Chem.*, 2009, **125**, 329.
- 9 R. Liu and X. Wang, *Polym. Degrad. Stab.*, 2009, **94**, 617.
- 10 M. E. Gouri, A. E. Bachiri, S. E. Hegazi, M. Rafik and A. E. Harfi, *Polym. Degrad. Stab.*, 2009, **94**, 2101.
- 11 D. E. Fennell, S. Du, F. Liu, H. Liu and M. M. Häggblom, *Reference Module in Earth Systems and Environmental Sciences*, 2011, **6**, 135.

- 12 A. Polder, G. W. Gabrielsen, J. Ø. Odland, T. N. Savinova, A. Tkachev, K. B. Løken and J. U. Skaare, *Sci. Total. Environ.*, 2008, **391**, 41.
- 13 I. Watanabe and S. Sakai, *Environ. Int.*, 2003, **29**, 665.
- 14 S. Takahashi, S. Sakai and I. Watanabe, *Chemosphere*, 2006, **64**, 234.
- 15 M. H. G. Berntssen, A. Maage, K. Julshamn, B. E. Oeye and A.-K. Lundebye, *Chemosphere*, 2011, **83**, 95.
- 16 O. Hutzinger and H. Thoma, *Chemosphere*, 1987, **16**, 1877.
- 17 R. Dumler, D. Lenoir, H. Thoma and O. Hutzinger. *Chemosphere*, 1990, **20**, 1867.
- 18 P. Wexler, *Encyclopedia of Toxicology*, Academic Press, New York, 3rd edn, 1992.
- 19 E. Çakmakçı and A. Güngör, *Polym. Degrad. Stab.*, 2013, **98**, 927.
- 20 S. Gaan, G. Sun, K. Hutches and M. H. Engelhard, *Polym. Degrad. Stab.*, 2008, **93**, 99.
- 21 W. Wu and C. Q. Yang, *Polym. Degrad. Stab.*, 2006, **91**, 2541.
- 22 D. Price, L. K. Cunliffe, K. J. Bullett, T. R. Hull, G. J. Milnes, J. R. Ebdon, B. J. Hunt and P. Joseph, *Polym. Degrad. Stab.*, 2007, **92**, 1101.
- 23 J. Chen, S. Liu and J. Zhao, *Polym. Degrad. Stab.*, 2011, **96**, 1508.
- 24 I. Veen and J. Boer, *Chemosphere*, 2012, **88**, 1119.
- 25 D. Hoang, J. Kim and B. N. Jang, *Polym. Degrad. Stab.*, 2008, **93**, 2042.
- 26 L. L. Pan, G. Y. Li, Y. C. Su and J. S. Lian, *Polym. Degrad. Stab.*, 2012, **97**, 1801.
- 27 L. Qian, L. Ye, Y. Qiu and S. Qu, *Polymer*, 2011, **52**, 5486.
- 28 H. Ma and Z. Fang, *Thermochim. Acta*, 2012, **543**, 130.
- 29 M. Remko, M. Swart and F. M. Bickelhaupt, *Bioorgan. Med. Chem.*, 2006, **14**, 1715.
- 30 H. Maeda, T. Chiba, M. Tsuhako and H. Nakayama, *Chem. Pharm. Bull.* 2008, **56**, 1698.
- 31 H. Inoue, T. Yamada, H. Nakayama and M. Tsuhako, *Chem. Pharm. Bull.* 2006, **54**, 1397.
- 32 H. Inoue, T. Kawashita, H. Nakayama and M. Tsuhako, *Carbohydr. Res.* 2005, **340**, 1766.

- 33 F. M. S. Stekhoven, H. G. Swarts, J. J. D. Pont and S. L. Bonting, *Biochim. Biophys. Acta*, 1983, **736**, 73.
- 34 I. N. Smirnova, A. A. Baykov and S. M. Avaeva, *FEBS Lett.*, 1986, **206**, 121.
- 35 H. Hiraishi, T. Ohmagari, Y. Otsuka, F. Yokoi and A. Kumon, *Arch. Biochem. Biophys.*, 1997, **341**, 153.
- 36 H. Maki, M. Tsujito, H. Nariai and M. Mizuhata, *Magn. Reson. Chem.*, 2014, **52**, 69.
- 37 H. Maki, M. Tsujito, M. Sakurai, T. Yamada, H. Nariai and M. Mizuhata, *J. Solution Chem.*, 2013, **42**, 2104.
- 38 H. Maki, M. Tsujito and T. Yamada, *J. Solution Chem.*, 2013, **42**, 1063.
- 39 H. Maki, H. Nariai, T. Miyajima, *Polyhedron*, 2011, **30**, 903.
- 40 H. Maki, T. Yamada, H. Nariai, M. Watanabe, M. Sakurai and T. Miyajima, *Phosphorus Res. Bull.*, 2001, **12**, 149.
- 41 H. Maki, T. Miyajima, S. Ishiguro, H. Nariai, I. Motooka, M. Sakurai and M. Watanabe, *Phosphorus Res. Bull.*, 1996, **6**, 9.
- 42 H. Maki, T. Miyajima, M. Sakurai, M. Watanabe, *Phosphorus Res. Bull.*, 1995, **5**, 149.
- 43 M. Sakurai and M. Watanabe, *Phosphorus Res. Bull.*, 1992, **2**, 39.
- 44 M. Komiya, T. Miyajima, M. Sakurai, S. Sato and M. Watanabe, *Phosphorus Res. Bull.*, 1992, **2**, 33.
- 45 G. Kura and T. Tsukuda, *Polyhedron*, 1993, **12**, 865.
- 46 G. Kura, *Polyhedron*, 1991, **10**, 697.
- 47 G. Kura, T. Nakashima and F. Oshima, *J. Chromatogr. A.*, 1987, **219**, 385.
- 48 F. Coleman and A. Erxleben, *Polyhedron*, 2012, **48**, 104.
- 49 G. Kura, *Polyhedron*, 1987, **6**, 531.
- 50 Y. Wang, W. Xiao, J. W. Mao, H. Zhou, Z. Q. Pan, *J. Mol. Struct.*, 2013, **1036**, 361.
- 51 G. Kura, *Bull. Chem. Soc. Jpn.* 1987, **60**, 2857.
- 52 M. Watanabe, M. Hinatase, M. Sakurai and S. Sato, *Gypsum & Lime*, 1991, **232**, 146.

- 53 H. Ootaki, *Denki Kagaku*, 1976, **44**, 151.
- 54 G. Gran, *Acta. Chem. Scand.*, 1950, **4**, 559.
- 55 G. Gran, *Analyst*, 1952, **77**, 661.
- 56 H. Nariai, I. Motooka, Y. Nakaji and M. Tshako, *Bull. Chem. Soc. Jpn.*, 1987, **60**, 1337.
- 57 R. N. Bell, L. F. Audrieth and O. F. Hill, *Ind. Eng. Chem.*, 1952, **44**, 568.
- 58 F. L. Conde and L. Prat, *Anal. Chim. Acta.*, 1957, **16**, 473.
- 59 A. L. Van Geet, *Anal. Chem.* 1968, **40**, 2227.
- 60 S. Braun, H. -O. Kalinowski and S. Berger, *150 and More Basic NMR Experiments: a practical course*, WILEY-VCH, Weinheim, 1998, chap. 5.2.
- 61 S. Braun, H. -O. Kalinowski and S. Berger, *150 and More Basic NMR Experiments: a practical course*, WILEY-VCH, Weinheim, 1998, pp.263.
- 62 M. Sakurai and M. Watanabe, *J. Mater. Sci.*, 1994, **29**, 4897.
- 63 M. Watanabe, M. Sakurai, S. Sato and H. Mori, *Gypsum & Lime*, 1992, **239**, 245.
- 64 M. Yuliana, C. T. Truong, L. H. Huynh, Q. P. Ho and Y. Ju, *LWT-Food Sci. Technol.*, 2014, **55**, 621.
- 65 C. Lee, J. Chen, W. Chang and I. Shiah, *Fluid Phase Equilibr.*, 2013, **343**, 30.
- 66 K. Chenab and D. Xue, *CrystEngComm*, 2012, **14**, 8068.
- 67 M. Watanabe, S. Sato and K. Wakasugi, *Bull. Chem. Soc. Jpn.*, 1990, **63**, 1243.
- 68 M. Watanabe, M. Sakurai, M. Hinatase and S. Sato, *J. Mater. Sci.*, 1992, **279**, 743.
- 69 U. Schülke, *Z. Anorg. Allg. Chem.*, 1968, **360**, 231.
- 70 V. M. Galogaža, E. A. Prodan, S. I. Pytlev, D. Skala, I. Ristić and L. Obradovic, *Thermochim. Acta*, 1986, **97**, 11.
- 71 J. W. Akitt, *NMR and Chemistry: An Introduction to Modern NMR Spectroscopy*, Chapman & Hall, London, 3rd edn, 1992. Chap. 2.1.
- 72 H. Maki, Y. Ueda and H. Nariai, *J. Phys. Chem. B*, 2011, **115**, 3571.

- 73 G. M. Chans, E. L. Moyano and M. T. Baumgartner, *J. Mol. Struct.*, 2014, **1059**, 176.
- 74 A. Arrieta, H. Jiao, A. Spannenberg and D. Michalik, *Tetrahedron*, 2013, **69**, 8872.
- 75 W. Schilf, B. Kamieński and K. Užarević, *J. Mol. Struct.*, 2013, **1031**, 211.
- 76 I. Alkorta, F. Blanco and J. Elguero, *Tetrahedron*, 2010, **66**, 5071.
- 77 A. Lyčka, Š. Frebort and N. Almonasy, *Tetrahedron Lett.*, 2008, **49**, 4213.
- 78 V. L. Júnior, M. G. Constantino, G. V. J. Silva, Á. C. Neto, C. F. Tormena, *J. Mol. Struct.*, 2007, **828**, 54.
- 79 A. B. Kudryavtsev and W. Linert, *Physico-chemical Applications of NMR: A Practical Guide*, World Scientific Publishing Co. Pte. Ltd., Singapore, 1996, chap. 4.
- 80 J. W. Akitt, *NMR and Chemistry: An Introduction to Modern NMR Spectroscopy*, Chapman & Hall, London, 3rd edn, 1992, chap. 5.
- 81 J. W. Akitt, *NMR and Chemistry: An Introduction to Modern NMR Spectroscopy*, Chapman & Hall, London, 3rd edn, 1992, pp.139.
- 82 A. B. Kudryavtsev and W. Linert, *Physico-chemical Applications of NMR: A Practical Guide*, World Scientific Publishing Co. Pte. Ltd., Singapore, 1996, pp.145.
- 83 D. Ray, A. Pramanik and N. Guchhait, *J. Photoch. Photobio. A*, 2014, **274**, 33.
- 84 B. K. Paul, A. Samanta, S. Kar and N. Guchhait, *J. Photoch. Photobio. A*, 2010, **214**, 203.
- 85 E. Kleinpeter, A. Koch, G. Fischer and C.-P. Askolin, *J. Mol. Struct.*, 1997, **435**, 65.
- 86 A. Lledós and J. Bertrán, *J. Mol. Struct-Theochem*, 1985, **120**, 73.
- 87 A. Lledós and J. Bertrán, *Tetrahedron Lett.*, 1981, **22**, 775.
- 88 L. Antonov, *Tautomerism: Methods and Theories*, WILEY-VCH, Weinheim, 2014.
- 89 T. Miyajima, H. Maki, M. Sakurai, S. Sato and M. Watanabe, *Phosphorus Res. Bull.*, 1993, **3**, 31.
- 90 S. Oh, G. Kawamura, H. Muto and A. Matsuda, *Solid State Ionics*, 2012, **225**, 223.
- 91 M. Yamada and I. Homma, *ChemPhysChem*, 2004, **5**, 724.

Table 1. Logarithmic first protonation constants of various $\text{cP}_4\text{O}_{12-n}(\text{NH})_n^{4-}$ ($n = 0, 3, 4$)^a determined by potentiometric titrations, $T = 25.0 \pm 0.5$ °C, $I = 0.10$ (NaNO₃).

Ligand	log K_{H}
$\text{cP}_4\text{O}_{12}^{4-}$	1.79 ± 0.01
$\text{cP}_4\text{O}_9(\text{NH})_3^{4-}$	3.09 ± 0.01
$\text{cP}_4\text{O}_8(\text{NH})_4^{4-}$	3.73 ± 0.01

^aThe errors given are equimultiple the standard deviation resulting from the nonlinear least squares calculations.

Table 2. Logarithmic first protonation constants and intrinsic ³¹P NMR chemical shifts of $\text{cP}_4\text{O}_{12-n}(\text{NH})_n^{4-}$ ($n = 0, 2, 3, 4$)^a determined by the pH profiles of ³¹P NMR chemical shifts^b of the anions in aqueous solutions^c, $T = 25.0 \pm 1.0$ °C, $I = 0.10$ (NaNO₃).

Ligand		log K_{H}	δ_{L} (ppm)	δ_{HL} (ppm)
$\text{cP}_4\text{O}_{12}^{4-}$	–O–PO ₂ –O–	1.75 ± 0.03	-20.43 ± 0.01	-20.60 ± 0.03
<i>trans</i> – $\text{cP}_4\text{O}_{10}(\text{NH})_2^{4-}$	–O–PO ₂ –NH–	2.59 ± 0.03	-8.79 ± 0.01	-9.63 ± 0.04
$\text{cP}_4\text{O}_9(\text{NH})_3^{4-}$	–O–PO ₂ –NH–	3.11 ± 0.01	-7.87 ± 0.01	-9.29 ± 0.01
	–NH–PO ₂ –NH–	3.07 ± 0.01	-1.47 ± 0.01	0.10 ± 0.01
$\text{cP}_4\text{O}_8(\text{NH})_4^{4-}$	–NH–PO ₂ –NH–	3.70 ± 0.03	-0.61 ± 0.01	0.01 ± 0.01

^aThe errors given are equimultiple the standard deviation resulting from the nonlinear least squares calculations. ^b Referenced to external 85% H₃PO₄. ^c In the absence of D₂O for field-frequency locking.

Figure captions

Fig. 1. ^{31}P NMR spectra of $\text{Na}_4\text{cP}_4\text{O}_9(\text{NH})_3\cdot\text{H}_2\text{O}$ aqueous solutions in the absence of ^1H decoupling.

(top): before pH-controlled recrystallization (2% purity), (bottom): after pH-controlled recrystallization of two times (95% purity). All resonances are singlets. Insets show the enlargement of the signals due to the non-equivalent phosphorus nuclei in $\text{cP}_4\text{O}_9(\text{NH})_3$ molecule. The details about pH-controlled recrystallization and NMR peak assignment are given in the text.

Fig. 2. Potentiometric titration curves of the protonation for $\text{cP}_4\text{O}_{12-n}(\text{NH})_n^{4-}$ ($n = 0, 3, 4$) at $25.0 \pm 0.5^\circ\text{C}$ and $I = 0.10$ (NaNO_3). (\circ); $\text{cP}_4\text{O}_{12}^{4-}$, (\square); $\text{cP}_4\text{O}_9(\text{NH})_3^{4-}$, (\diamond); $\text{cP}_4\text{O}_8(\text{NH})_4^{4-}$. Solid line refers to the calculated curve by the use of the pertinent parameters of $\log K_{\text{H}} = 1.79$ ($\text{cP}_4\text{O}_{12}^{4-}$), 3.09 ($\text{cP}_4\text{O}_9(\text{NH})_3^{4-}$), 3.73 ($\text{cP}_4\text{O}_8(\text{NH})_4^{4-}$), respectively, see eqn (4).

Fig. 3. ^{31}P NMR chemical shifts of $\text{cP}_4\text{O}_{12-n}(\text{NH})_n^{4-}$ ($n = 0, 2, 3, 4$) as a function of pH at $25.0 \pm 1.0^\circ\text{C}$ and $I = 0.10$ (NaNO_3). Solid lines refer to the calculated curves by the use of the pertinent parameters of Table 2, see eqn (6). (\circ); $\text{cP}_4\text{O}_{12}^{4-}$ ($\text{O}-\underline{\text{P}}-\text{O}$), (\blacktriangledown); *trans*- $\text{cP}_4\text{O}_{10}(\text{NH})_2^{4-}$ ($\text{O}-\underline{\text{P}}-\text{N}$), (\blacksquare); $\text{cP}_4\text{O}_9(\text{NH})_3^{4-}$ ($\text{O}-\underline{\text{P}}-\text{N}$), (\square); $\text{cP}_4\text{O}_9(\text{NH})_3^{4-}$ ($\text{N}-\underline{\text{P}}-\text{N}$), (\diamond); $\text{cP}_4\text{O}_8(\text{NH})_4^{4-}$ ($\text{N}-\underline{\text{P}}-\text{N}$).

Fig. 4. Variation of $\log K_{\text{H}}$ values of $\text{cP}_3\text{O}_{9-n}(\text{NH})_n^{3-}$ ($n = 0-3$) and $\text{cP}_4\text{O}_{12-n}(\text{NH})_n^{4-}$ ($n = 0, 2, 3, 4$) at 25.0°C against the number of imino groups which constitute the ligand molecules. Open symbols, $\text{cP}_3\text{O}_{9-n}(\text{NH})_n^{3-}$ ($n = 0-3$); filled symbols, $\text{cP}_4\text{O}_{12-n}(\text{NH})_n^{4-}$ ($n = 0, 2, 3, 4$). The $\log K_{\text{H}}$ values for $\text{cP}_4\text{O}_{12-n}(\text{NH})_n^{4-}$ ($n = 0, 3, 4$), for $\text{cP}_4\text{O}_{12-n}(\text{NH})_n^{4-}$ ($n = 2$), and for

$\text{cP}_3\text{O}_{9-n}(\text{NH})_n^{3-}$ ($n = 0-3$) were referred from Table 1, Table 2, and Table S2 (reference 42), respectively.

Fig. 5. Additivity rule for the intrinsic ^{31}P NMR chemical shifts of $\text{cP}_4\text{O}_{12-n}(\text{NH})_n^{4-}$ ($n = 0, 2, 3, 4$). (left): deprotonated ligands, (right): protonated ligands. Filled symbols in the lower and higher magnetic field indicate the intrinsic chemical shifts of $\text{cP}_4\text{O}_{12-n}(\text{NH})_n^{4-}$ ($n = 0, 4$) which is the reference values for the “ $\delta_{\text{L}}^{\text{N}}$ ”, “ $\delta_{\text{L}}^{\text{O}}$ ”, “ $\delta_{\text{HL}}^{\text{N}}$ ”, and “ $\delta_{\text{HL}}^{\text{O}}$ ”, respectively. The details for the additivity rule are given in the text and eqns (8) and (9).

Fig. 6. TG-DTA curves of $\text{Na}_4\text{cP}_4\text{O}_8 \cdot 4\text{H}_2\text{O}$ (left), $\text{Na}_4\text{cP}_4\text{O}_8(\text{NH})_4 \cdot 2\text{H}_2\text{O}$ (middle) and $\text{Na}_4\text{cP}_4\text{O}_9(\text{NH})_3 \cdot \text{H}_2\text{O}$ (right) at $10\text{ }^\circ\text{C} \cdot \text{min}^{-1}$ in an air atmosphere (initial mass 20.0 mg).

Fig. 7. X-ray diffraction patterns of $\text{Na}_4\text{cP}_4\text{O}_9(\text{NH})_3 \cdot \text{H}_2\text{O}$ (left) and $\text{Na}_4\text{cP}_4\text{O}_8(\text{NH})_4 \cdot 2\text{H}_2\text{O}$ (right) at room temperature and after heat treatment at several temperature in an air atmosphere. The peaks marked with closed circles (\bullet) are due to $\text{Na}_3\text{cP}_3\text{O}_9$, and the peaks marked with closed reverse triangles (\blacktriangledown) are due to $\text{Na}_4\text{cP}_4\text{O}_{12}$.

Scheme 1. Preparation of $\text{Na}_4\text{cP}_4\text{O}_8(\text{NH})_4 \cdot 2\text{H}_2\text{O}$ for the synthesis of $\text{Na}_4\text{cP}_4\text{O}_9(\text{NH})_3 \cdot \text{H}_2\text{O}$.

Scheme 2. Synthesis of $\text{Na}_4\text{cP}_4\text{O}_9(\text{NH})_3 \cdot \text{H}_2\text{O}$ by the hydrolysis of $\text{Na}_4\text{cP}_4\text{O}_8(\text{NH})_4 \cdot 2\text{H}_2\text{O}$.

Scheme 3. Purification of $\text{Na}_4\text{cP}_4\text{O}_9(\text{NH})_3 \cdot \text{H}_2\text{O}$ by pH-controlled recrystallization.

Scheme 4. Lactam-lactim tautomerism of $\text{cP}_4\text{O}_8(\text{NH})_4^{4-}$ anion. (top): completely dissociated state, (bottom): completely protonated state.

Scheme 5. Protonation equilibrium model of $\text{cP}_4\text{O}_9(\text{NH})_3^{4-}$ anion which contains lactam-lactim tautomerism.

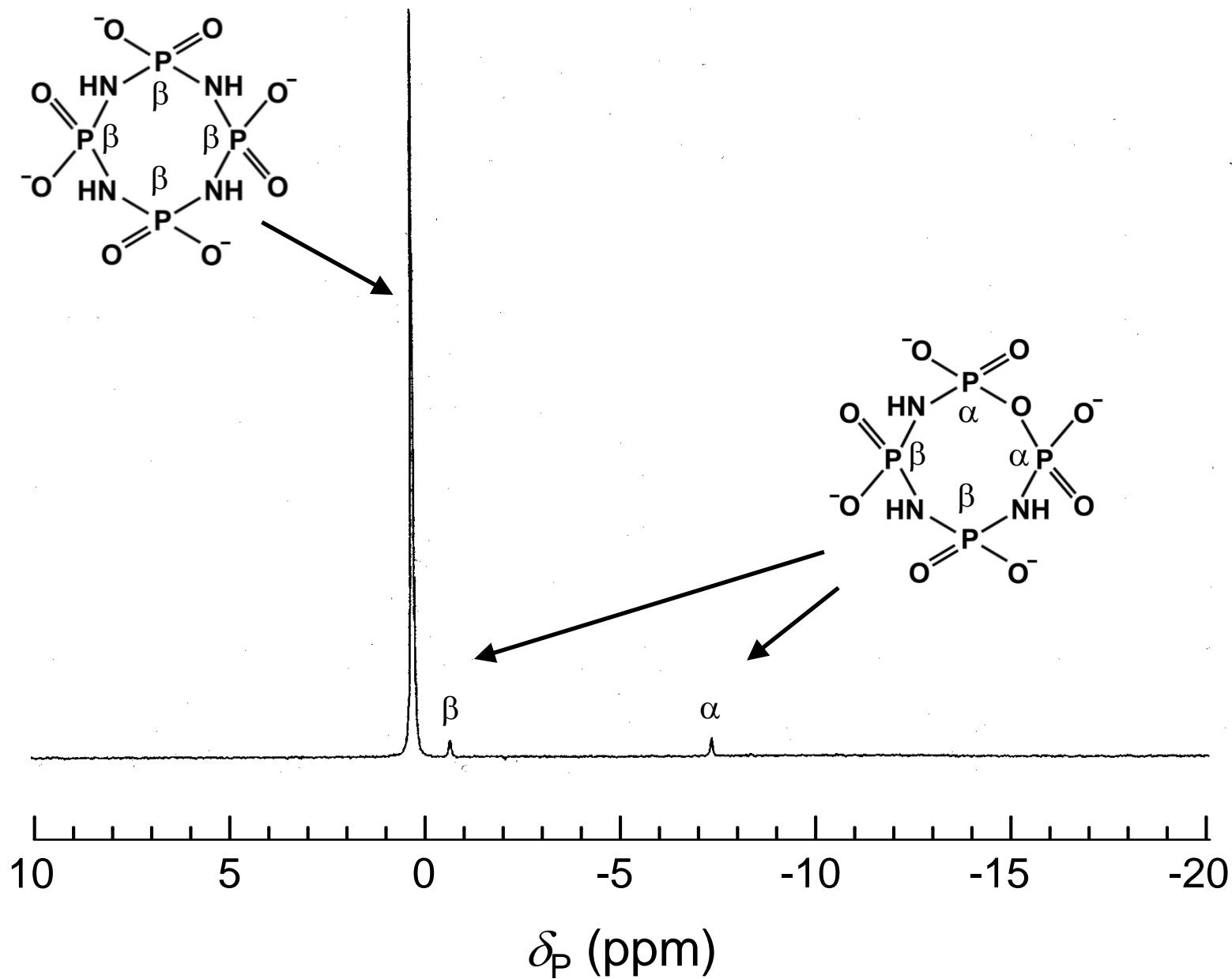


Fig.1(top)

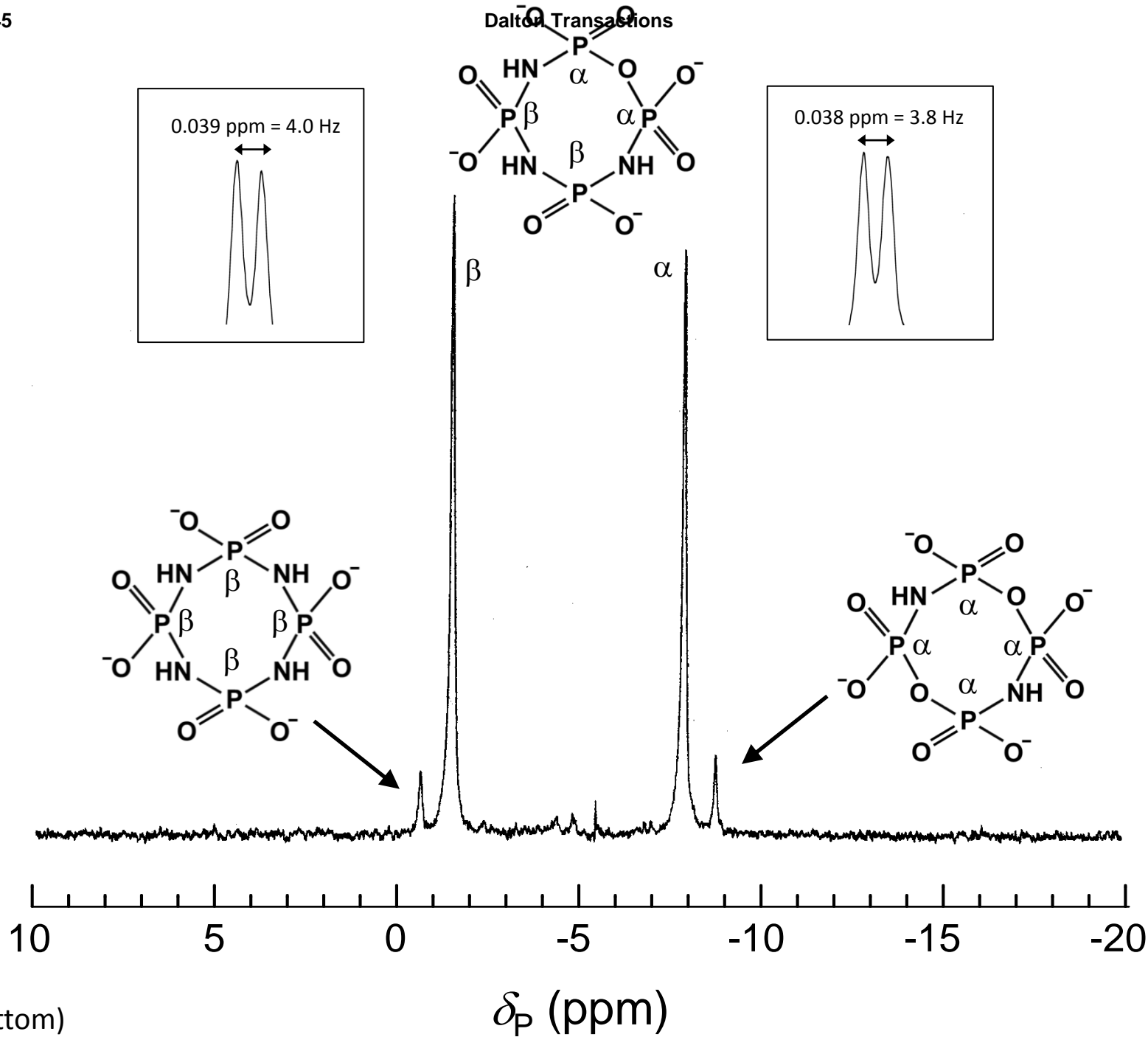


Fig.1(bottom)

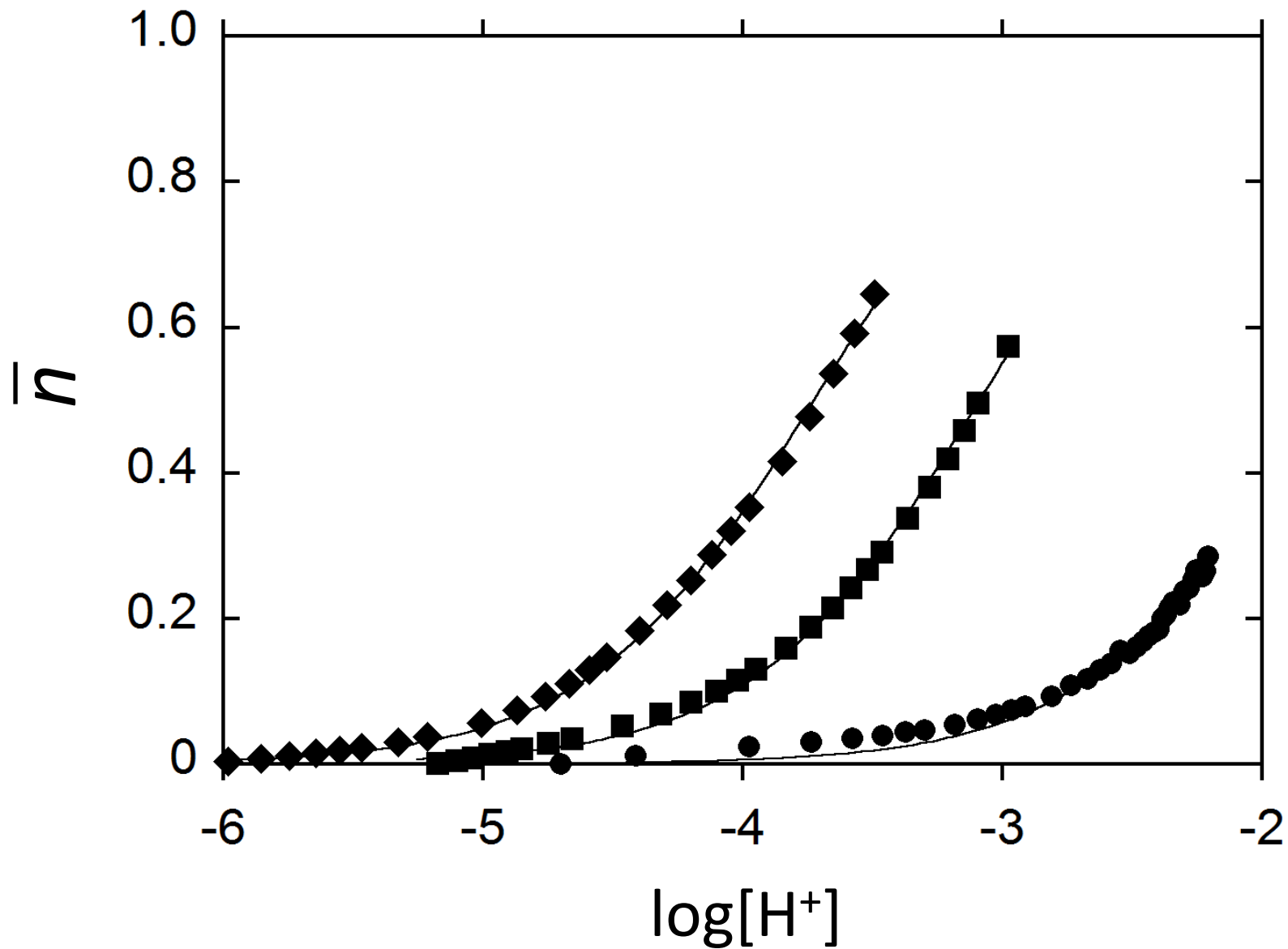


Fig.2

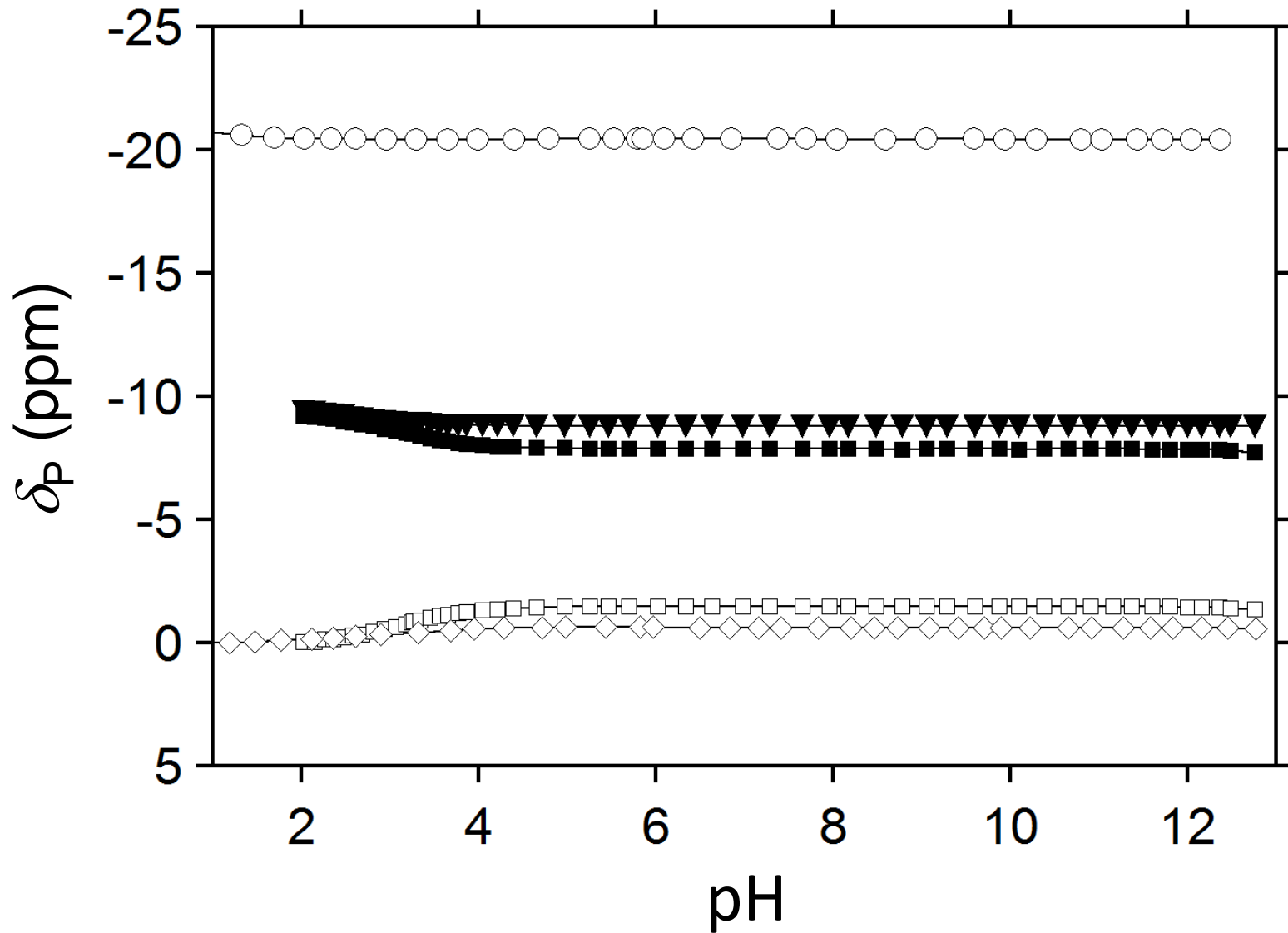


Fig.3

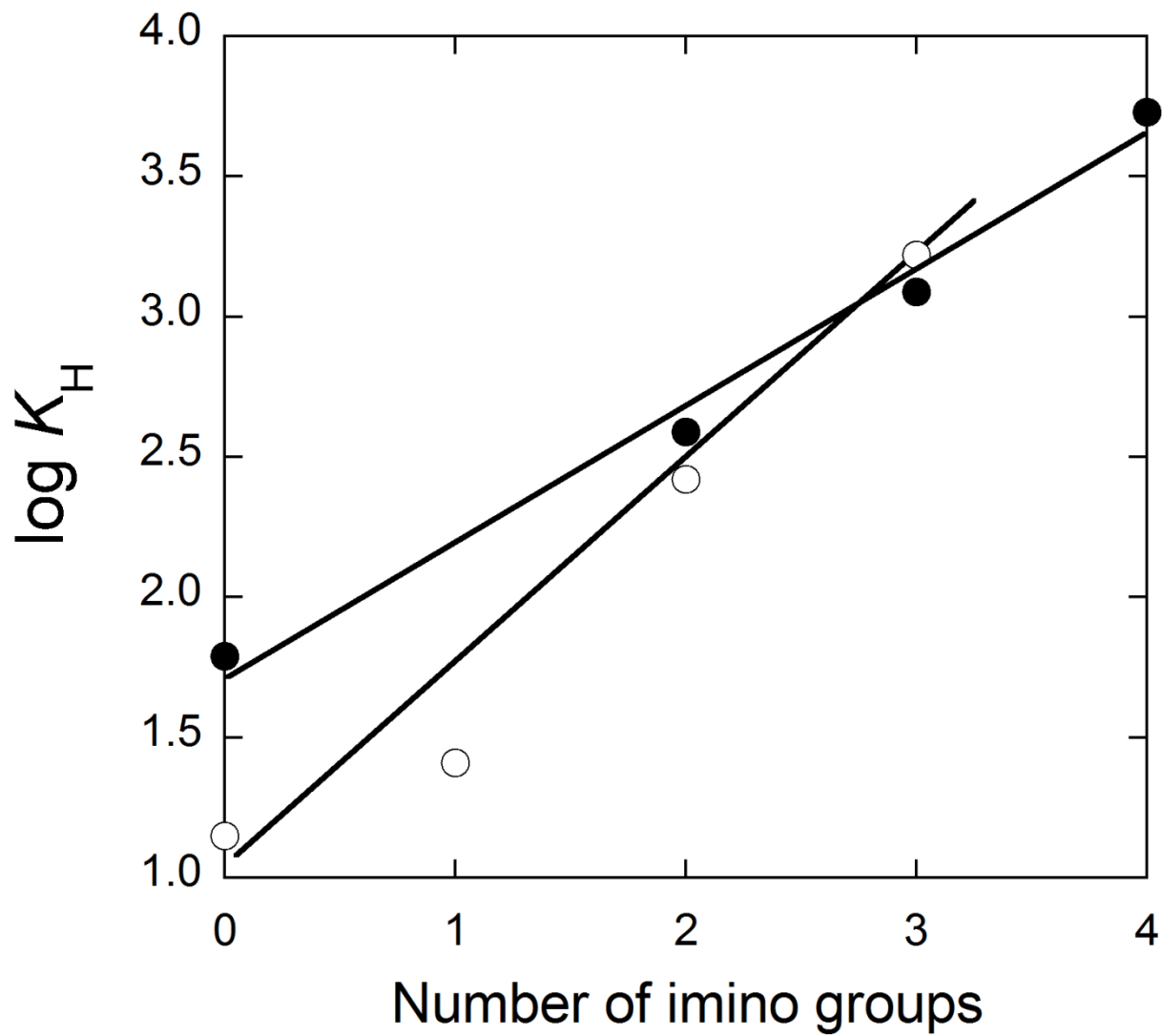


Fig.4

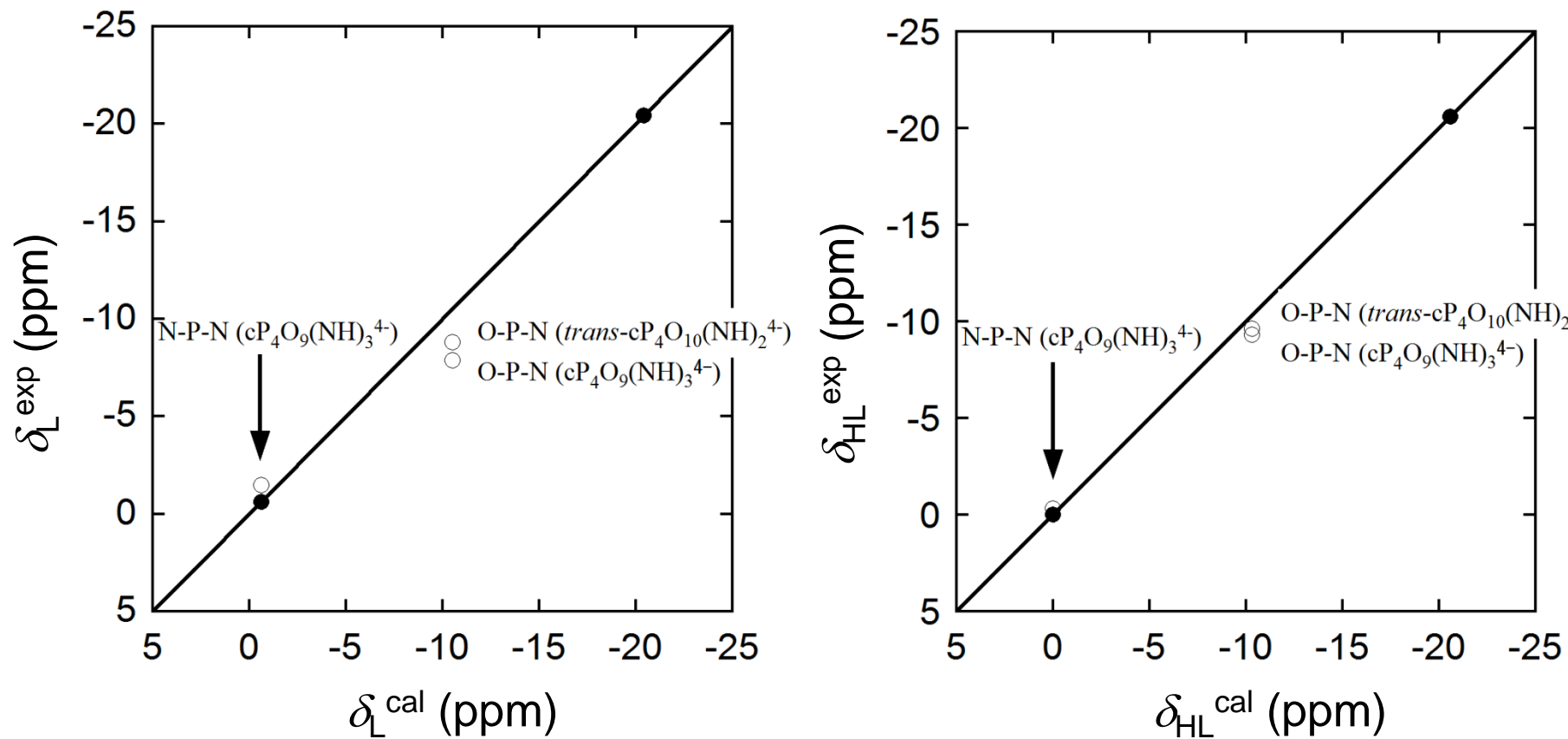


Fig.5

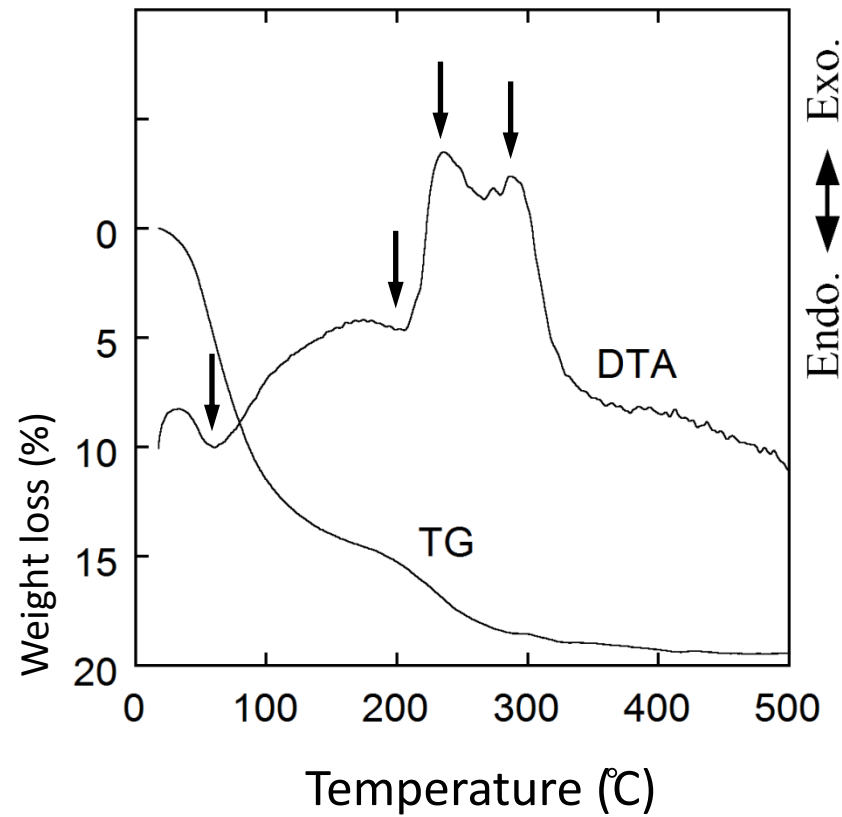
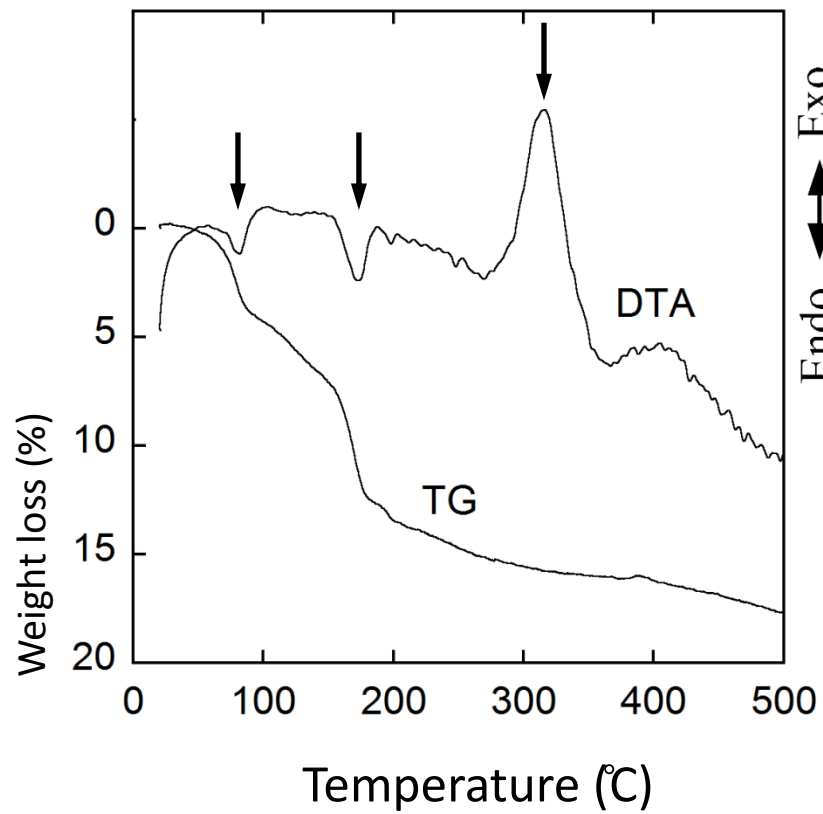


Fig.6

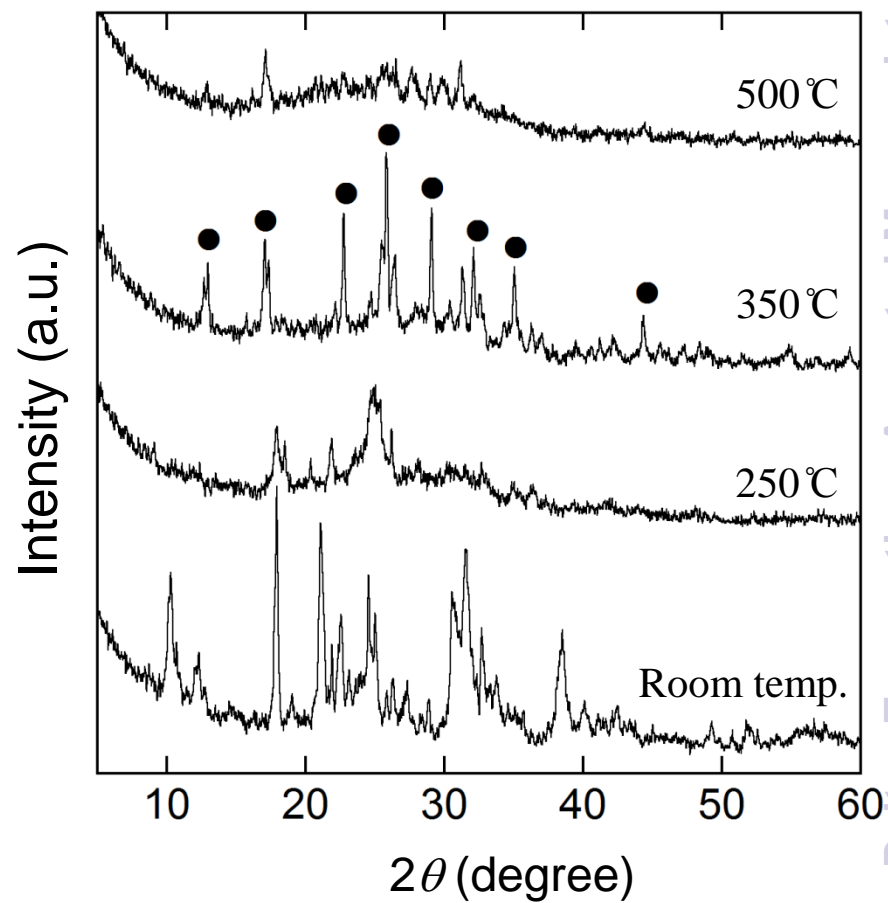
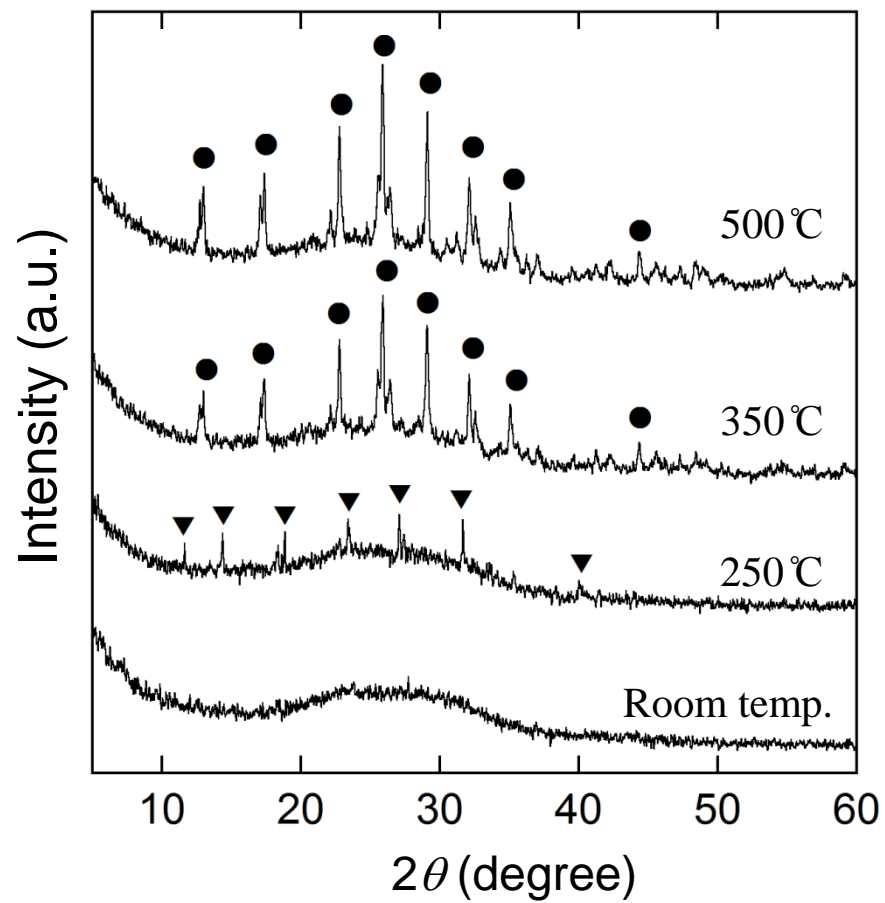
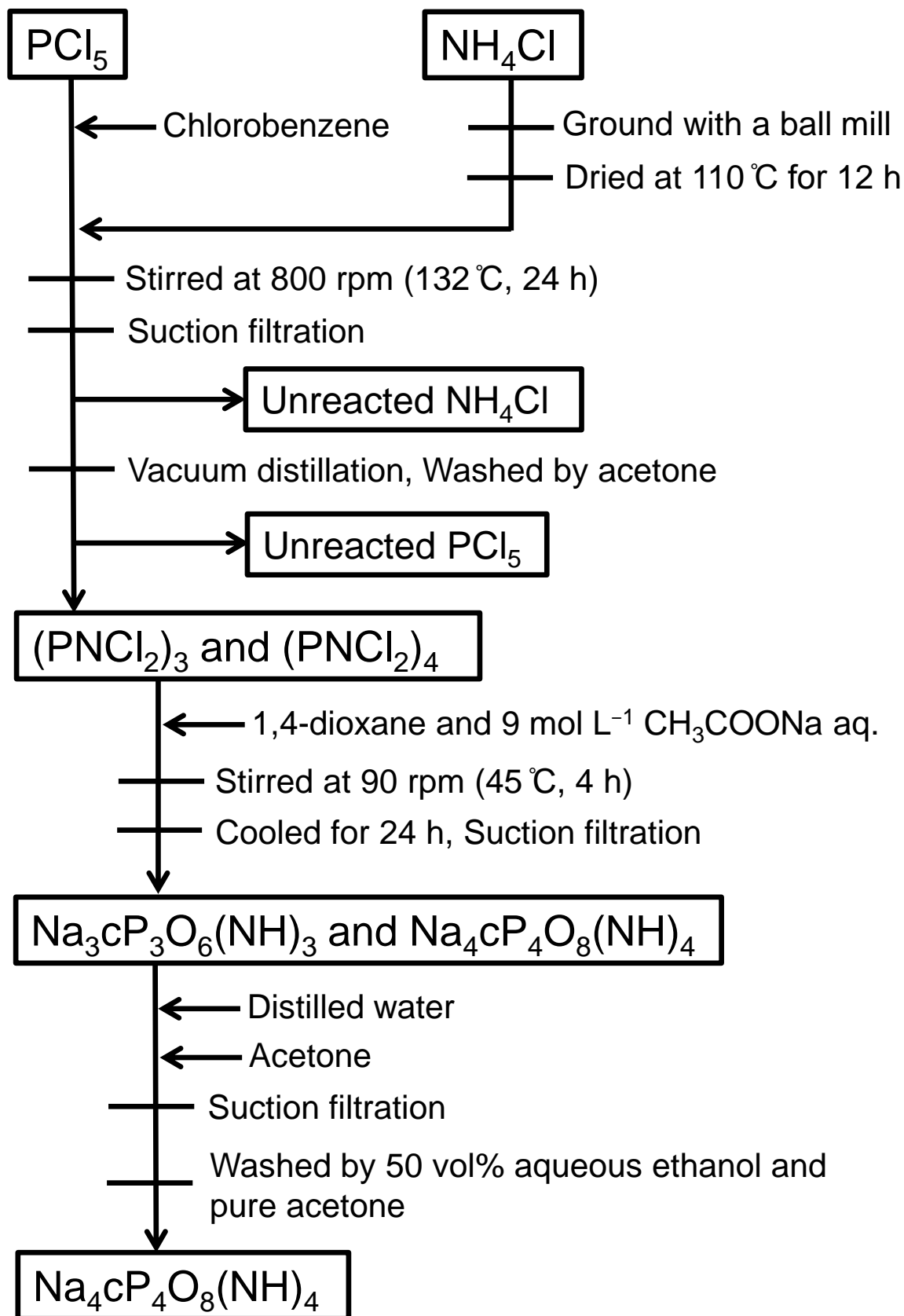
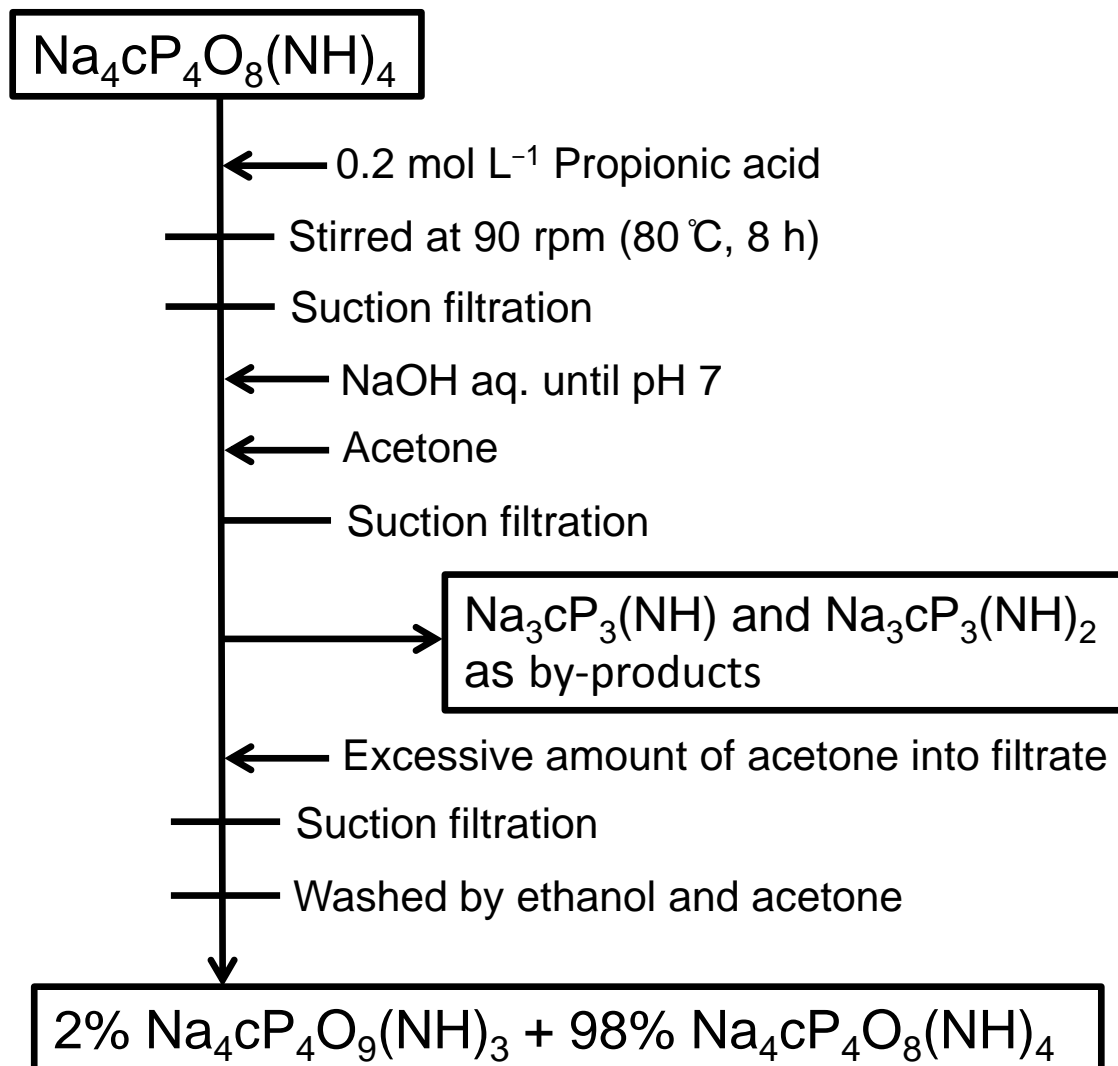
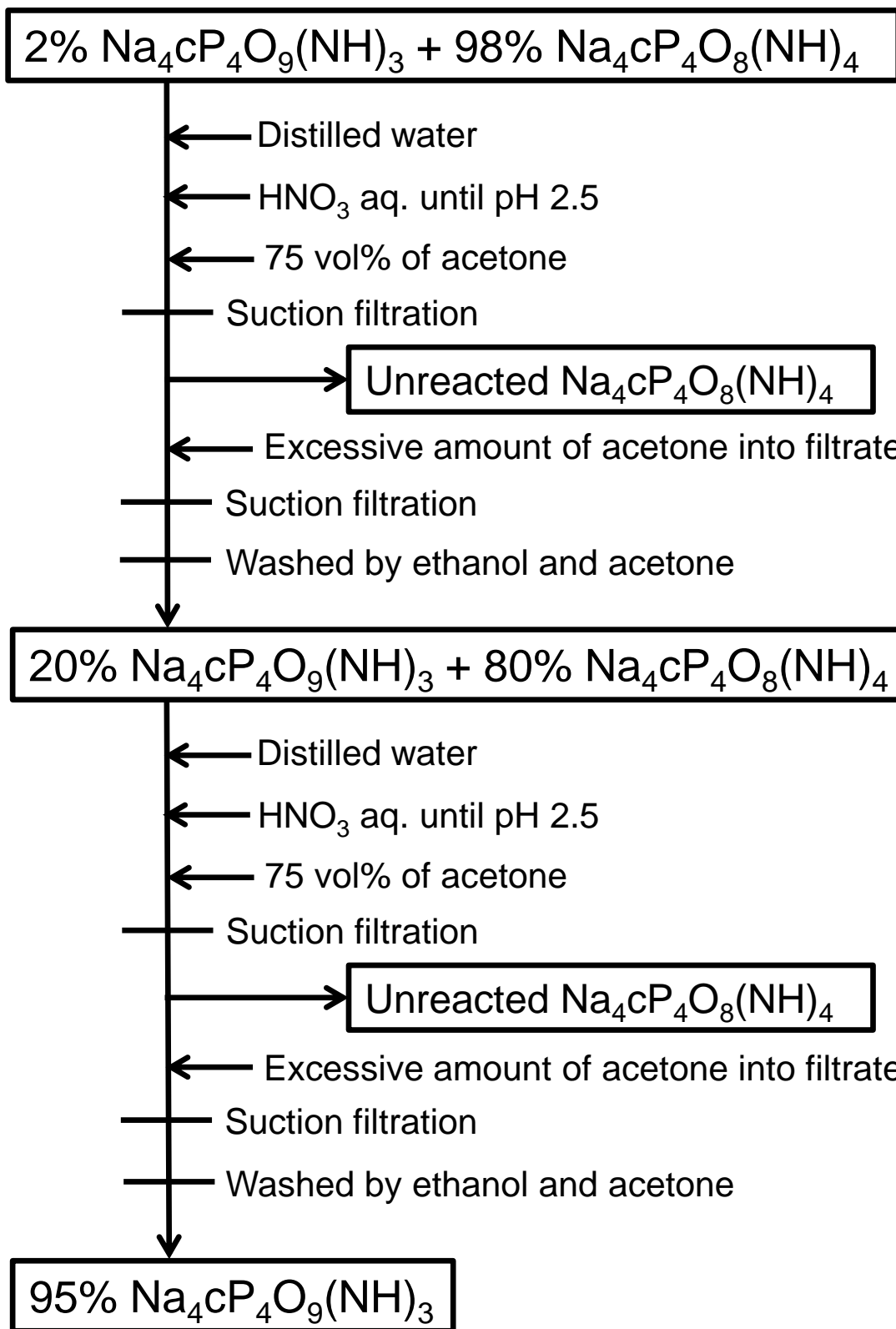


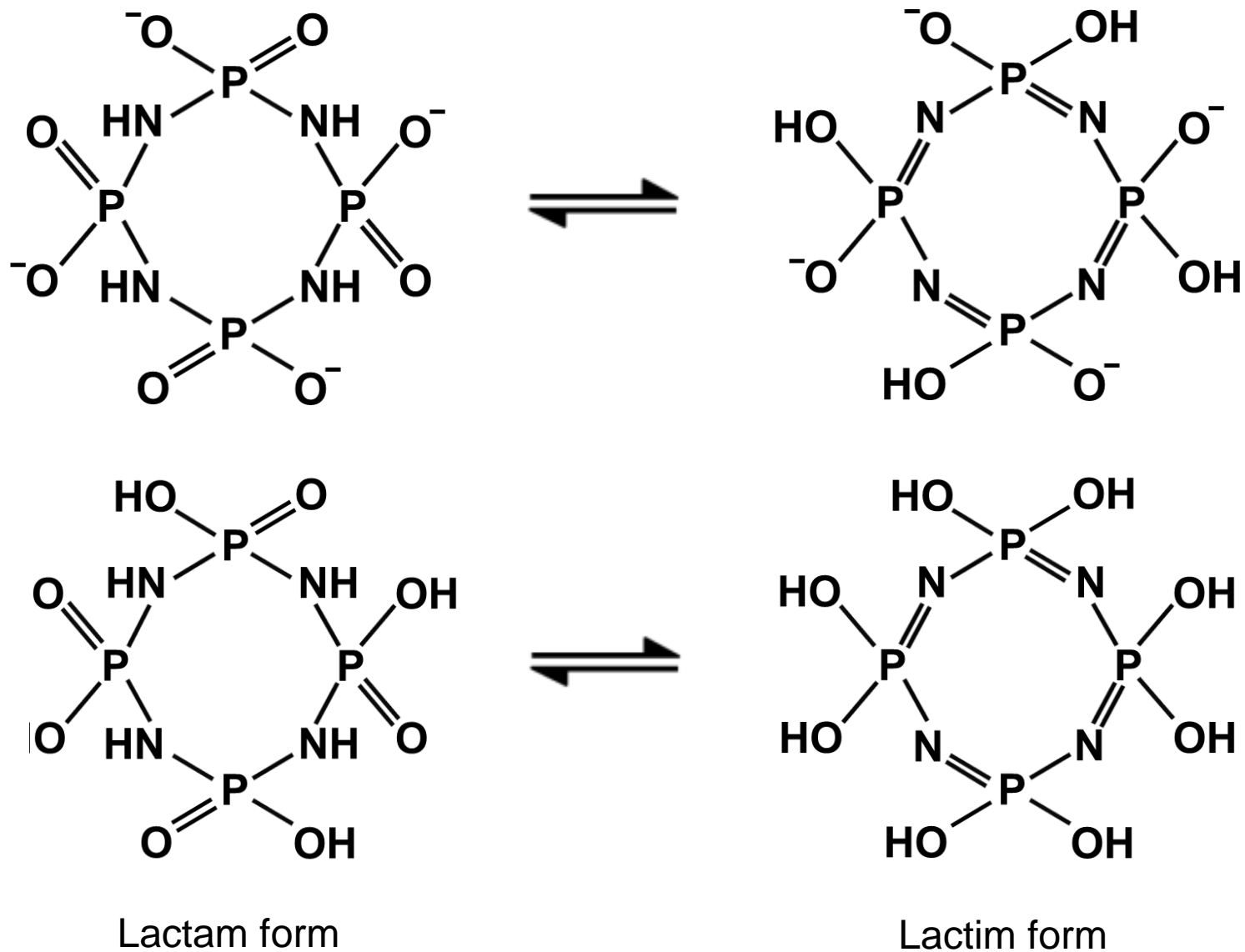
Fig.7

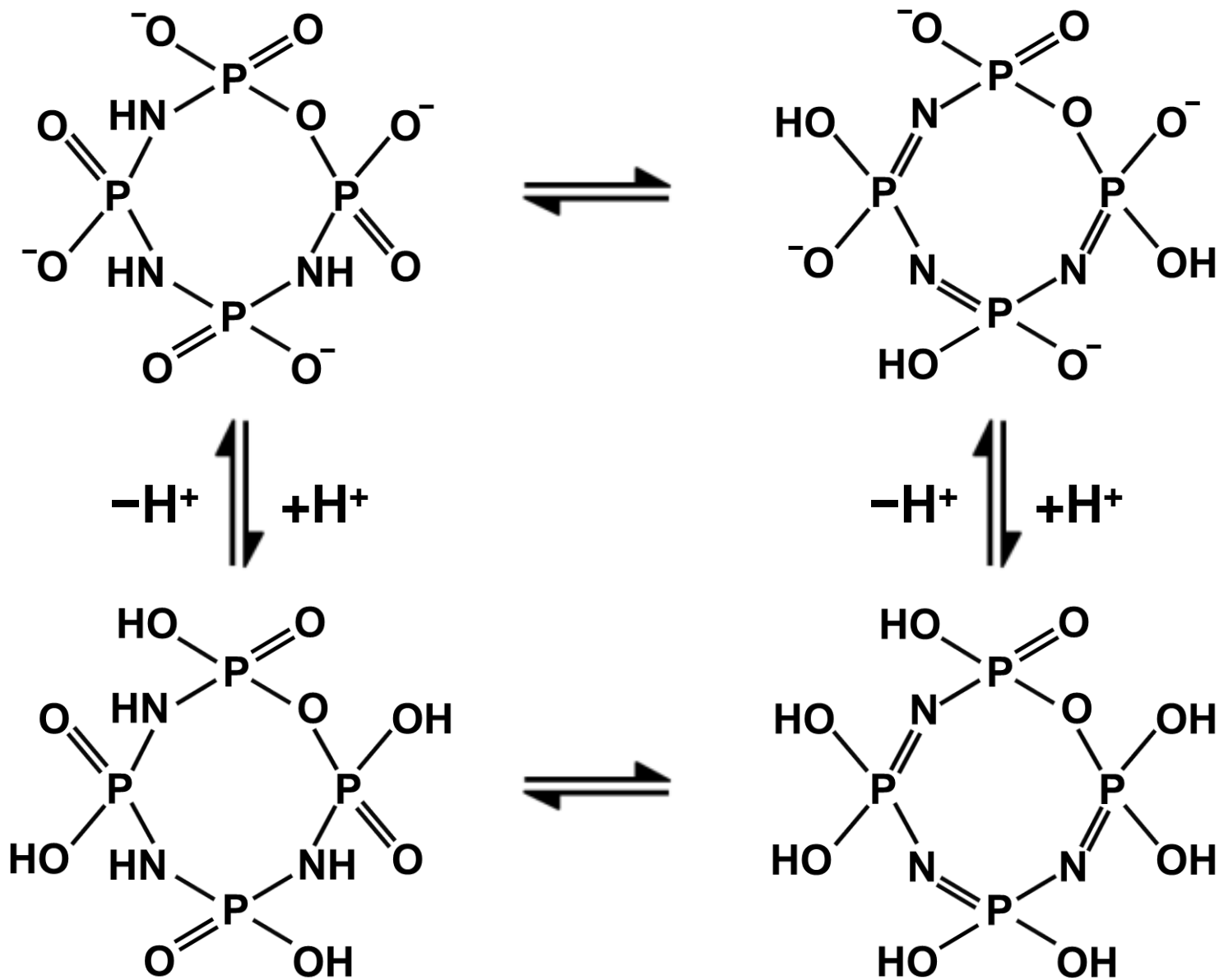


Scheme 1









Scheme 5

